



**NORTH SPIRIT LAKE AREA
(MAIN AND NORTH BLOCKS)**

**Ontario Airborne Geophysical Surveys
Magnetic and Electromagnetic Data
Geophysical Data Set 1056**

Ontario Geological Survey
Ministry of Northern Development and Mines
Willet Green Miller Centre
933 Ramsey Lake Road
Sudbury, Ontario, P3E 6B5
Canada

TABLE OF CONTENTS

CREDITS.....	2
DISCLAIMER.....	2
CITATION	2
NOTE.....	2
1) INTRODUCTION.....	3
2) SURVEY LOCATION AND SPECIFICATIONS.....	4
3) AIRCRAFT, EQUIPMENT AND PERSONNEL.....	7
4) DATA ACQUISITION.....	10
5) DATA COMPILATION AND PROCESSING	12
6) MICROLEVELLING AND GSC LEVELLING OF THE MAGNETIC DATA	21
7) FINAL PRODUCTS.....	32
8) QUALITY ASSURANCE AND QUALITY CONTROL.....	35
REFERENCES.....	40
APPENDIX A TESTING AND CALIBRATION	42
APPENDIX B PROFILE ARCHIVE DEFINITION.....	46
APPENDIX C ANOMALY ARCHIVE DEFINITION	52
APPENDIX D KEATING CORRELATION ARCHIVE DEFINITION	54
APPENDIX E GRID ARCHIVE DEFINITION.....	55
APPENDIX F GEOTIFF AND VECTOR ARCHIVE DEFINITION.....	56
APPENDIX G TDEM PARAMETER TABLE DEFINITION.....	57
APPENDIX H HALF-WAVE ARCHIVE DEFINITION.....	61
APPENDIX I MULTICOMPONENT MODELING.....	62

CREDITS

This survey is part of the Far North Geological Mapping Initiative (FNGMI), funded by the Ontario Government.

List of accountabilities and responsibilities:

- Jack Parker, Senior Manager, Precambrian Geoscience Section, Ontario Geological Survey (OGS), Ministry of Northern Development and Mines (MNDM) – accountable for the airborne geophysical survey projects, including contract management
- Stephen Reford, Vice President, Paterson, Grant & Watson Limited (PGW), Toronto, Ontario, FNGMI Geophysicist under contract to MNDM, responsible for the airborne geophysical survey project management, quality assurance (QA) and quality control (QC)
- Tom Watkins, FNGMI Data Manager, Information & Marketing Services Section, Ontario Geological Survey, MNDM – manage the project-related hard copy products
- Desmond Rainsford, FNGMI Data Manager, Precambrian Geoscience Section, Ontario Geological Survey, MNDM – manage the project-related digital products
- Fugro Airborne Surveys, Geoterrex office, Ottawa, Ontario - data acquisition and data compilation.

DISCLAIMER

To enable the rapid dissemination of information, this digital data has not received a technical edit. Every possible effort has been made to ensure the accuracy of the information provided; however, the Ontario Ministry of Northern Development and Mines does not assume any liability or responsibility for errors that may occur. Users may wish to verify critical information.

CITATION

Information from this publication may be quoted if credit is given. It is recommended that reference be made in the following form:

Ontario Geological Survey 2007. Ontario airborne geophysical surveys, magnetic and electromagnetic data, North Spirit Lake area; Ontario Geological Survey, Geophysical Data Set 1056.

NOTE

Chief and Council of First Nation communities within and adjacent to this Far North Geological Mapping Initiative survey area request that you contact the closest First Nation community if you carry out any work in these areas. You are also encouraged to determine that the area you are working in does not represent an area of overlap where traditional

activities are carried out by more than one community. Contact information for First Nation communities is obtained at the following website sponsored by Indian and Northern Affairs Canada: http://pse2-esd2.ainc-inac.gc.ca/FNProfiles/FNProfiles_home.htm

1) INTRODUCTION

The Far North Geological Mapping Initiative is a 3-year program of the Ontario Ministry of Northern Development and Mines that commenced in 2005. The Initiative is intended to provide a better understanding of the mineral resource potential of targeted areas in Ontario's Far North through the collection and analysis of geoscience data and through the marketing of these data to the minerals industry. The initiative incorporates the following elements:

- Airborne geophysical surveys/remote sensed imagery
- Create new compilation maps based on analysis of existing and new geoscience data.
- New "feet-on-the-ground" geological bedrock and Quaternary mapping.
- Geochemical surveys and surficial mapping.
- Purchase proprietary geoscience data from the private sector.
- Aboriginal community engagement.

The geophysical component of the Initiative requires flying new airborne magnetic and electromagnetic surveys over various greenstone belts in the Far North and producing the results in digital and hardcopy formats suitable for publication.

The airborne survey contracts were awarded through a Request for Proposal and Contractor Selection process. The system and contractor selected for each survey area were judged on many criteria, including the following:

- applicability of the proposed system to the local geology and potential deposit types
- aircraft capabilities and safety plan
- experience with similar surveys
- QA/QC plan
- capacity to acquire the data and prepare final products in the allotted time
- price-performance.

2) SURVEY LOCATION AND SPECIFICATIONS

The North Spirit Lake survey area is located in north-western Ontario (Figure 1). The survey area is focussed on the North Spirit Lake greenstone belt. The North Spirit Lake greenstone belt is part of a long, narrow chain of supracrustal units along the north and northeast side of the Berens River Subprovince. The supracrustal rocks are cut at an angle of a few degrees by a major transcurrent fault (Bear Head fault) between Favourable Lake and North Spirit Lake; the North Spirit greenstone belt is defined as that part of the supracrustal belt lying south of the Bear Head fault. The North Spirit greenstone belt extends 100 km south-easterly attaining a width of about 15 km at North Spirit Lake where subsidiary arms of the belt radiate west and northeast. The belt consists of felsic to ultramafic metavolcanic rocks, clastic and chemical metasedimentary rocks and a variety of felsic to ultramafic intrusions. The bedrock exposure in the northern and western parts of the survey area is very good. Significant concentrations of overburden are found at one location. The area south of North Spirit Lake, extending to the shore of McDowell Lake, hosts undifferentiated till, composed mainly of a sand to silty sand matrix, as well as glaciolacustrine deposits (sand, gravely sand, gravel) and an eastnortheast-striking esker (gravel and sand). The overburden covers mainly the greenstone belt. Limited drilling indicates that the overburden is generally less than 5 m thick (increasing to 10 m to the southeast), with a maximum thickness of 23 m.

The GEOTEM® 1000 time-domain electromagnetic (90 Hz base frequency) and magnetic system, mounted on a fixed wing platform, was selected by MNDM to conduct the survey.

The airborne survey and noise specifications for the North Spirit Lake survey area are as follows:

a) traverse line spacing and direction

Main Block (A)

- flight line spacing is 200 m
- flight line direction is 40° - 220°
- maximum deviation from the nominal traverse line location could not exceed 50 m over a distance greater than 2000 m.
- minimum separation between two adjacent lines could be no smaller than 150 m or larger than 250 m.

North Block (B)

- flight line spacing is 200 m
- flight line direction is 130° - 310°
- maximum deviation from the nominal traverse line location could not exceed 50 m over a distance greater than 2000 m.
- minimum separation between two adjacent lines could be no smaller than 150 m or larger than 250 m.

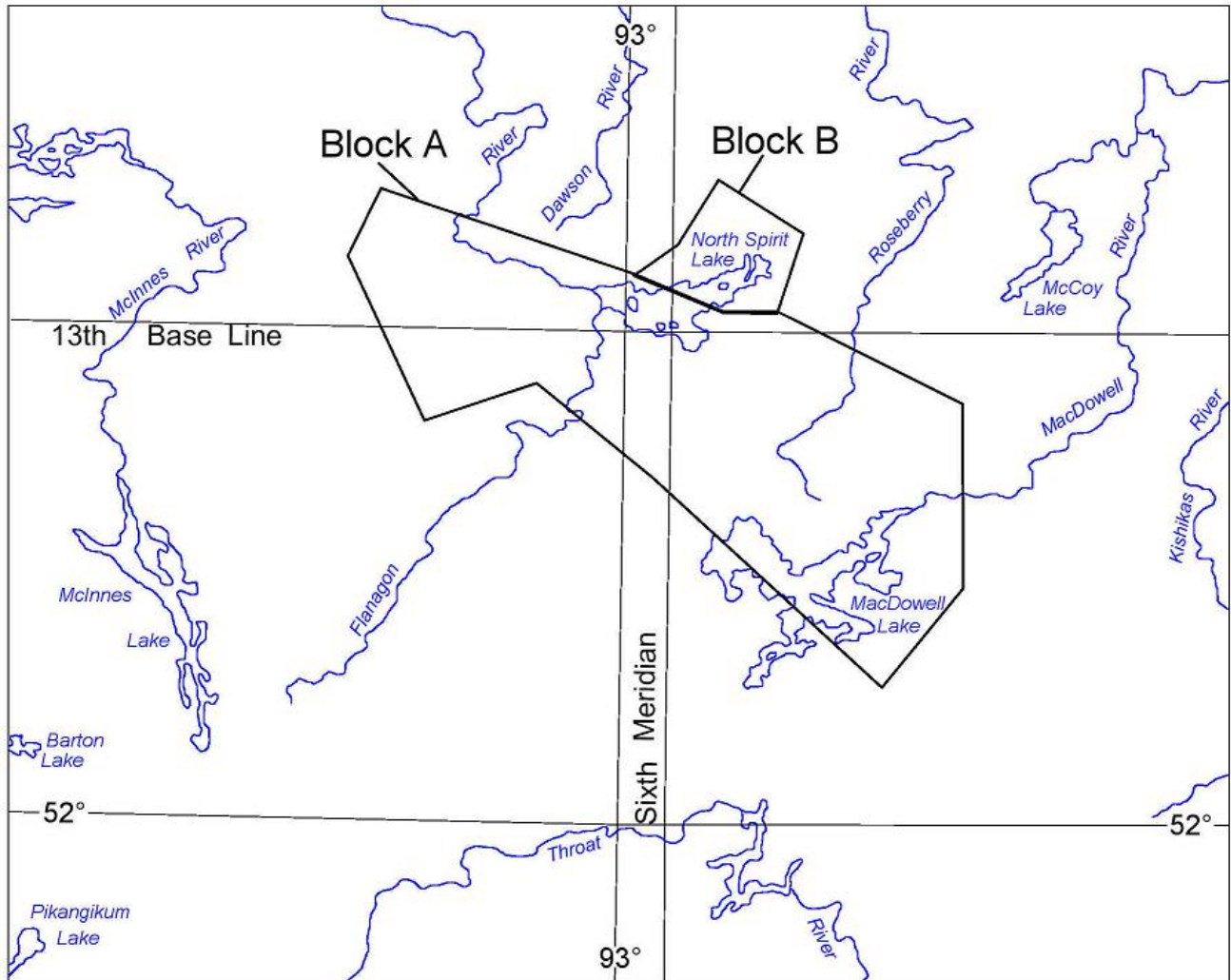


Figure 1: North Spirit Lake area GEOTEM[®] 1000 survey over Block A (Main) and Block B (North).

- b) control line spacing and direction
 - at regular 1500 m intervals, perpendicular to the flight line direction.
 - along each survey boundary (if not parallel to the flight line direction).
 - maximum deviation from the nominal control line location could not exceed 50 m over a distance greater than 2000 m.
- c) terrain clearance of the EM receiver bird
 - nominal terrain clearance is 75 m.
 - altitude tolerance limited to ± 15 m over 3000 m, except in areas of severe topography.

- d) aircraft speed
 - nominal aircraft speed is 65 m/sec.
 - aircraft speed tolerance limited to ± 10 m/sec, except in areas of severe topography.
- e) magnetic diurnal variation
 - could not exceed a maximum deviation of 3 nT peak-to-peak over a 60 second chord.
- f) magnetometer noise envelope
 - in-flight noise envelope could not exceed 0.2 nT, for straight and level flight.
 - heading error could not to exceed 2 nT.
 - base station noise envelope could not exceed 0.1 nT.
- g) EM receiver noise envelope
 - the noise envelope could not exceed:
 - dB/dt X ± 2800 pT/s over a distance exceeding 3000 m.
 - dB/dt Z ± 2800 pT/s over a distance exceeding 3000 m.

3) AIRCRAFT, EQUIPMENT AND PERSONNEL

Aircraft and Geophysical On-Board Equipment

Aircraft: CASA C-212 twin turbo-prop (GEOTEM[®] 1000 system)
Operator: FUGRO AIRBORNE SURVEYS
Registration: C-FDKM
Survey Speed: 125 knots / 145 mph / 65m/sec.
Magnetometer: Scintrex Cs-2 single cell cesium vapour, towed-bird installation, sensitivity of 0.1 nT, sampling rate = 0.1 sec., ambient range 20,000 to 100,000 nT. The general noise envelope was kept below 0.11 nT. Nominal sensor height of 70 metres above ground.

Electromagnetic system: GEOTEM[®] 1000 multicoil system
CASA (C-FDKM)
Transmitter: vertical axis loop of 231 m²
number of turns: 6
nominal height above ground of 120 metres
mean current of ~525 amperes
mean dipole moment of ~7.0 x 10⁵ Am²
Receiver : multicoil system (X, Y and Z) with a final recording rate of 4 samples/second, for the recording of 20 channels of X, Y and Z-coil data; nominal height above ground of 75 metres, placed 131 m behind the centre of the transmitter loop
Base frequency: 90 Hz
Pulse delay: 100 μs
Point value: 43.4 μs
Flights 1 to 8:
Pulse width: 2160 μs
Off-time: 3295 μs
Window mean delay times in milliseconds from the end of the pulse
channel 1: -2.000 channel 11: 0.908
channel 2: -1.566 channel 12: 1.082
channel 3: -1.001 channel 13: 1.277
channel 4: -0.437 channel 14: 1.494
channel 5: -0.003 channel 15: 1.711
channel 6: 0.192 channel 16: 1.950
channel 7: 0.322 channel 17: 2.210
channel 8: 0.453 channel 18: 2.493
channel 9: 0.583 channel 19: 2.796
channel 10: 0.735 channel 20: 3.122

Flights 9 to 36:

Pulse width: 2244 μ s
Off-time: 3211 μ s
Window mean delay times in
milliseconds from the end of the pulse
channel 1: -2.062 channel 11: 0.824
channel 2: -1.606 channel 12: 0.998
channel 3: -1.042 channel 13: 1.193
channel 4: -0.499 channel 14: 1.410
channel 5: -0.065 channel 15: 1.627
channel 6: 0.152 channel 16: 1.866
channel 7: 0.282 channel 17: 2.126
channel 8: 0.412 channel 18: 2.409
channel 9: 0.542 channel 19: 2.712
channel 10: 0.672 channel 20: 3.038

Digital Acquisition: FUGRO AIRBORNE SURVEYS GeoDAS

Analogue Recorder: RMS GR-33, showing the total magnetic field at 2 vertical scales, the radar and barometric altimeters, X-coil and Z-coil channels 8, 15 and 20 of the filtered dB/dt and B Field data, dB/dt X, Y and Z raw channel 20 as well as B Field X and Z raw channel 20, the EM primary field from the X- and Y-coils, the power line monitor, the 4th difference of the magnetics, the X-coil earth's field and fiducials

Barometric Altimeter: Rosemount 1241M, sensitivity 1 foot, 1 sec. recording interval

Radar Altimeter: King, accuracy 2%, sensitivity one foot, range 0 to 2,500 feet, 1 sec. recording interval

Camera: Panasonic colour video, super VHS, model WV-CL302

Electronic Navigation: NovAtel OEM4 GPS receiver, 1 sec. recording interval, with a resolution of 0.00001 degree and an accuracy of ± 5 m. Real time differential correction was provided by Omnistar.

Base Station Equipment

Magnetometer: Scintrex CS-2 single cell cesium vapour, mounted in a magnetically quiet area, measuring the total intensity of the earth's magnetic field in units of 0.01 nT at intervals of 1 second, within a noise envelope of 0.10 nT

GPS Receiver: NovAtel OEM4, measuring all GPS channels, for up

to 12 satellites

Computer: Toshiba laptop

Converter: CF-1 SBBS

Field Office Equipment

Computers: Dell Inspiron Pentium 4 laptop with 120 GB hard drive and an external 300 GB Hard drive

Printer: Hewlett Packard Deskjet 690C

Hard Drive: Removable SCSI hard drive

Field Personnel

The following personnel were on-site during the acquisition program.

David Murray	Supervising Processor
Ron Wiseman	Geophysicist
Adam Jones	Geophysicist
Mark Morrison	Geophysicist Intern
Alan Capyk	Pilot
Darcy Wiens	Pilot
Brock Gorrell	Pilot
Paula McNeil	Pilot
Alex Meson	Pilot
Tom Hudgin	Pilot
Todd Boughner	Aircraft engineer
J.L. Daigle	Aircraft engineer
Shane Hanlon	Aircraft engineer
Jeff Robb	Aircraft engineer
Iaroslav Gorokhovski	Electronics technician
Dave Patzer	Electronics technician
Ahsan Aziz	Electronics technician

All above personnel are employees of Fugro Airborne Surveys.

4) DATA ACQUISITION

The town of Balmertown, Ontario was selected as the base of operation. The survey was carried out from November 4th, 2006 to January 28th, 2007, with various pre survey test flights being flown from October 21st, 2006 to October 27th, 2006. The area is covered by a total of 10,239 line kilometres of flying. The survey area, divided into two separate blocks (Main and North), was defined by a flight line direction selected to run perpendicular to the average trend of the local geological structures. A total of 470 survey lines were flown over the two blocks (391 over the Main Block and 79 over the North Block) with a separation of 200 metres. An additional 46 control lines were flown (33 over the Main Block and 13 over the North Block) perpendicular to the traverse lines at a separation of 1,500 metres or along the survey block boundaries.

General statistics

Pre-Survey test flight dates	October 21 st , 2006 to October 27 th , 2006
Survey dates	November 4 th , 2006 to January 28 th , 2007
Total Survey km	10,239 km
	Main Block = 9,298 km
	North Block = 941 km
Total flying hours	167.9 hours
Production hours	137.0 hours
Number of production days	26 days
Number of production flights	35 flights
Bad weather days	13 days
Testing and training	16.3 hours
Electronics maintenance	67days
Aircraft movement	23.1 hours
Aircraft maintenance	32 days *
Pilot training	5 days
Average production per flight	293 km
Average production per hour	75 km
Average production per day	394 km

* This total includes all days lost to an unscheduled wing x-ray scan, as ordered by the aircraft manufacturer in response to an incident in Sweden involving the same model aircraft.

The following tests and calibrations were performed prior to the commencement of the survey flying:

- Magnetometer lag check
- EM system lag check
- GPS navigation lag and accuracy check
- Altimeter calibration
- Magnetometer heading (cloverleaf) check.

These tests were flown from bases in Timmins or Ottawa, as part of the start-up procedures. The Reid-Mahaffy Airborne Geophysical Test Site Survey was flown prior to mobilization to Balmertown.

Details of these tests and their results are given in Appendix A.

After each flight, all analogue records were examined as a preliminary assessment of the noise level of the recorded data. Altimeter deviations from the prescribed flying altitudes were also closely examined as well as the magnetic diurnal activity, as recorded on the base station.

All digital data were verified for validity and continuity. The data from the aircraft and base station were transferred to the PC's hard disk and the eternal backup hard disk. Basic statistics were generated for each parameter recorded. These included the minimum, maximum and mean values, the standard deviation and any null values located. All recorded parameters were edited for spikes or datum shifts, followed by final data verification via an interactive graphics screen with on-screen editing and interpolation routines.

The quality of the GPS navigation was controlled on a daily basis by recovering the flight path of the aircraft. The correction procedure employs the raw ranges from the base station to create improved models of clock error, atmospheric error, satellite orbit, and selective availability. These models are used to improve the conversion of aircraft raw ranges to aircraft position.

Checking all data for adherence to specifications was carried out in the field by the Fugro Airborne Surveys field geophysicist.

5) DATA COMPILATION AND PROCESSING

Personnel

The following personnel were involved in the compilation of data and creation of the final products:

Michael Pearson	Manager of the Compilation Department
David Murray	Supervising Processor
Jean Lemieux	Chief Geophysicist
Stuart Stevenson	Geophysicist
Mark Morrison	Geophysicist Intern

Base Maps

Base maps of the survey area were supplied by the Ontario Ministry of Northern Development and Mines.

Projection Description

Datum:	NAD83 (Canada)
Ellipsoid:	GRS80
Projection:	UTM (Zone 15N)
Central Meridian:	93° W
False Northing:	0 m
False Easting:	500,000 m
Scale factor:	0.9996

Processing of Base Station Data

The recorded magnetic diurnal base station data is reformatted and loaded into the OASIS database. After initial verification of the integrity of the data from statistical analysis, the appropriate portion of the data is selected to correspond to the exact start and end time of the flight. The data is then checked and corrected for spikes using a fourth difference editing routine. Following this, interactive editing of the data is done, via a graphic editing tool, to remove events caused by man-made disturbances. A small noise filter, such as a 5 point running average, is then applied if necessary. The final processing step consists of extracting the long wavelength component of the diurnal signal, through low pass filtering, to be subtracted from the airborne magnetic data as a pre-levelling step.

Processing of the Positioning Data (GPS)

The raw GPS data from both the mobile (aircraft) and base station are recovered. Positions are initially recalculated from the recorded raw data range in flight. Post-flight recalculation of the fixes from the raw ranges rather than using the fixes which are recorded directly in flight, improves on the positional accuracy, as it eliminates possible time tag errors that can result during the real-time processing required to get from the range data to the fixes directly within the receiver. Differential corrections are then applied to the aircraft fixes using the recorded base station data. The resulting differentially corrected latitudes and longitudes are then converted from the WGS-84 spheroid to UTM metres. A point to point speed calculation is then done from the final X,Y coordinates and reviewed as part of the quality control. The flight data is then cut back to the proper survey line limits and a preliminary plot of the flight path is done and compared to the planned flight path to verify the navigation. The positioning data is then exported to the other processing files.

Processing of the Altimeter Data

The altimeter data, which includes the radar altimeter, the barometric altimeter and the GPS elevation values, after differential corrections, are checked and corrected for spikes using a fourth difference editing routine. A small noise filter, such as a 5 point running average, is then applied to the data. During periods of poor satellite visibility which may affect the resolution of the GPS elevation values, the barometric altimeter data is available to bridge over the bad segments. Following this, a digital terrain trace is computed by subtracting the radar altimeter values from the differentially corrected GPS elevation values. All resulting parameters are then checked, in profile form, for integrity and consistency, using a graphic viewing editor.

Processing of Magnetic Data

The data is reformatted and loaded into the OASIS database. After initial verification of the data by statistical analysis, the values are adjusted for system lag. The data is then checked and corrected for any spikes using a fourth difference editing routine and inspected on the screen using a graphic profile display. Interactive editing, if necessary, is done at this stage. Following this, the long wavelength component of the diurnal is subtracted from the data as a pre-levelling step. A preliminary grid of the values is then created and verified for obvious problems, such as errors in positioning or bad diurnal. Appropriate corrections are then applied to the data, as required. The International Geomagnetic Reference Field (IGRF) is then calculated from the 2005 model year extrapolated to 2007.05 at the aircraft elevation and removed from the corrected values.

Following this, the final levelling process is undertaken. This consists of calculating the positions of the control points (intersections of flight lines and tie lines), calculating the magnetic differences at the control points and applying a series of levelling corrections (combination of movements and compensations) to reduce the misclosures to zero. A new grid of the values is then created and checked for residual errors. Any gross errors detected are corrected in the profile database and the levelling process repeated. Residual errors are extracted from the

gridded values using the PGW microlevelling procedure (see section 6 - Microlevelling and GSC Levelling), and microlevelling corrections applied to the profile data

The “GSC-levelled” channel is used to prepare the magnetic grid. This residual magnetic field is gridded using the minimum curvature algorithm.

Second Vertical Derivative of the Residual Magnetics

The final grid of the residual magnetic field is then used as input to create the second vertical derivative. The calculation is done in the frequency domain by combining the transfer function of the second vertical derivative and a small low pass filter (designed using a Butterworth filter, see section 6 - Microlevelling and GSC Levelling) aimed at attenuating the high frequency signal enhanced by the second derivative operator, without aliasing the geological signal.

Keating Correlation Coefficients

Possible kimberlite targets are identified from the residual magnetic intensity data, based on the identification of roughly circular anomalies. This procedure is automated by using a known pattern recognition technique (Keating, 1995), which consists of computing, over a moving window, a first-order regression between a vertical cylinder model anomaly and the gridded magnetic data. Only the results where the absolute value of the correlation coefficient is above a threshold of 75% were retained. On the magnetic maps, the results are depicted as circular symbols, scaled to reflect the correlation value. The most favourable targets are those that exhibit a cluster of high amplitude solutions. Correlation coefficients with a negative value correspond to reversely magnetised sources.

The cylinder model parameters are as follows:

- Cylinder diameter: 200 m
- Cylinder length: infinite
- Overburden thickness: 5.3 m
- Magnetic inclination: 77.4° N
- Magnetic declination: 0.8° W
- Magnetization scale factor: 100
- Model window size: 14 (560 m x 560 m)
- Model window grid cell size: 40 m

The model computed using these parameters is shown in Figure 2.

It is important to be aware that other magnetic sources may correlate well with the vertical cylinder model, whereas some kimberlite pipes of irregular geometry may not. The user should study the magnetic anomaly that corresponds with the Keating symbols, to determine whether it does resemble a kimberlite pipe signature, reflects some other type of source or even noise in the data e.g. boudinage (beading) effect of the minimum curvature gridding. All available geological information should be incorporated in kimberlite pipe target selection.

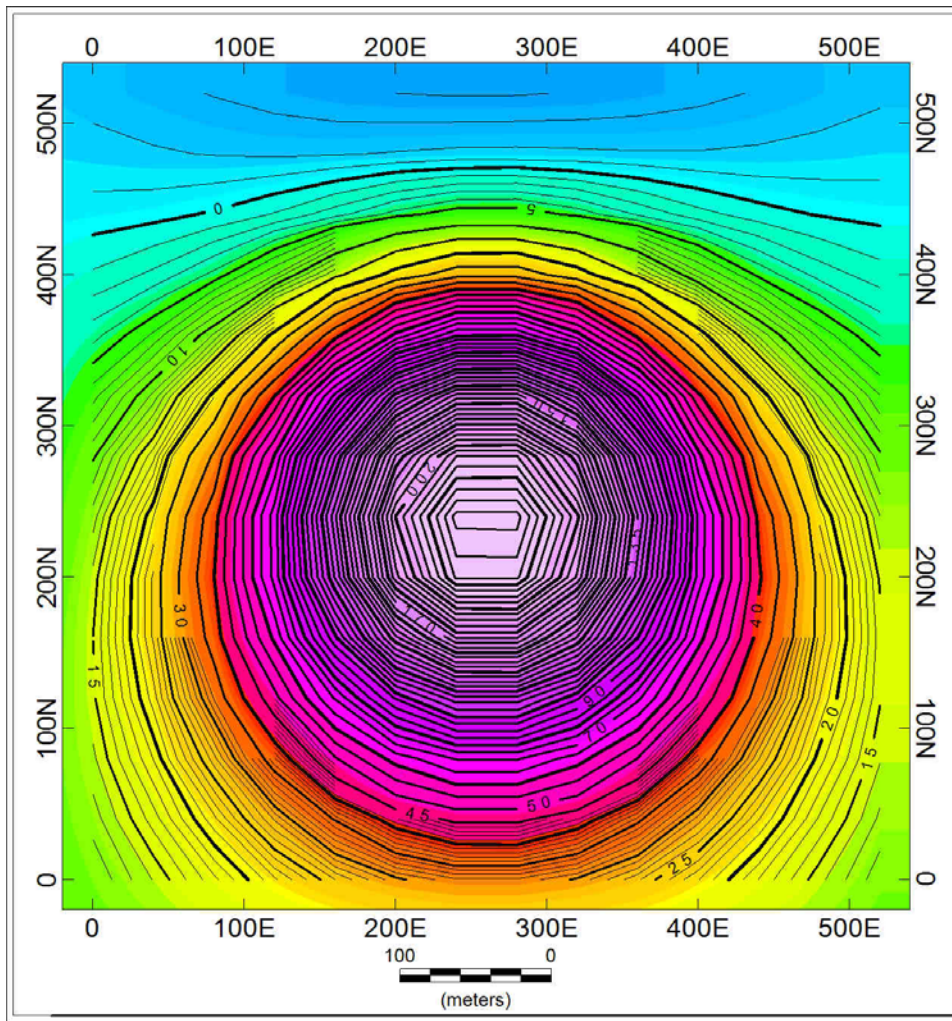


Figure 2: Vertical cylinder anomaly model used for Keating correlation on the North Spirit Lake survey. Grid cell interval is 40 m and contour interval is 1 nT.

Processing of the Electromagnetic Data

The data is reformatted and loaded into the OASIS database. After initial verification of the data by statistical analysis, the values are then adjusted for system lag. The next step is to check and correct each individual channel for system drift. Slightly different processing steps are applied to dB/dt and B-Field data.

For dB/dt data from all coil sets, from channels 1 to 5 (on-time) and 6 to 20 (off-time), are corrected for drift in flight form (prior to cutting the recorded data back to the correct line limits) by passing a low order polynomial function through the baseline minima along each channel, via a graphic screen display. The data is edited for residual spheric spikes by examining the decay pattern of each individual EM transient. Bad decays (i.e. not fitting a normal exponential function) are deleted and replaced by interpolation. Corrections are made in the X- and Z-coil data for low frequency, incoherent noise elements (that do not correlate from channel to channel) in the data, by analysing the decay patterns of channels 14 to 20 (OMEGA process). Noise filtering is done using

an adaptive filter technique based on time domain triangular operators. Using a 2nd difference value to identify changes in gradient along each channel, minimal filtering (in this case a 3 point convolution) is applied over the peaks of the anomalies, ranging in set increments up to a maximum amount of filtering in the resistive background areas (in this case 21 points for both the X-coil and the Z-coil data).

For B-Field data the processing stream is very similar to that of the regular dB/dt data. The lag adjustment used is the same, followed by the drift adjustments, spike editing for spheric events, and the correction for coherent noise. By nature, the B-Field data contains a higher degree of coherency of the noise that automatically gets eliminated (or considerably attenuated) than in the regular dB/dt, since the latter is the time derivative of the signal. Finally noise is filtered using an adaptive filter.

The introduction of the B-Field data stream, as part of the GEOTEM[®] system, provides the explorationist with a more effective tool for exploration in a broader range of geological environments and for a larger class of target priorities. The advantage of the B-Field data compared with the normal voltage data (dB/dt) are as follows:

- a) A broader range of target conductance that the system is sensitive to. (The B-Field is sensitive to bodies with conductance as great as 100,000 siemens);
- b) Enhancement of the slowly decaying response of good conductors;
- c) Suppression of rapidly decaying response of less conductive overburden;
- d) Reduction in the effect of spherics on the data;
- e) An enhanced ability to interpret anomalies due to conductors below thick conductive overburden;
- f) Reduced dynamic range of the measured response (easier data processing and display).

Figure 3 displays the calculated vertical plate response for the GEOTEM[®] signal for the dB/dt and B-Field. For the dB/dt response, you will note that the amplitude of the early channel peaks at about 25 siemens, and the late channels at about 250 siemens. As the conductance exceeds 1000 siemens the response curves quickly roll back into the noise level. For the B-Field response, the early channel amplitude peaks at about 80 siemens and the late channel at about 550 siemens. The projected extension of the graph in the direction of increasing conductance, where the response would roll back into the noise level, would be close to 100,000 siemens. Thus, a strong conductor, having a conductance of several thousand siemens, would be difficult to interpret on the dB/dt data, since the response would be mixed in with the background noise. However, this strong conductor would stand out clearly on the B-Field data, although it would have an unusual character, being a moderate to high amplitude response, exhibiting almost no decay.

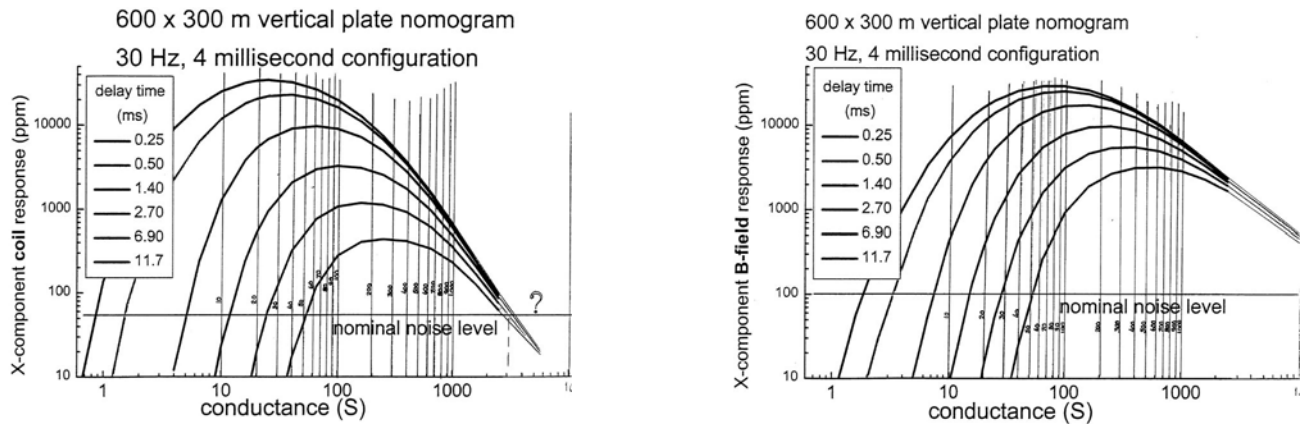


Figure 3: dB/dt vertical plate nomogram (left), B-field vertical plate nomogram (right).

In theory, the response from a super conductor (50,000 to 100,000 siemens) would be seen on the B-Field data as a low amplitude, non-decaying anomaly, not visible in the off-time channels of the dB/dt stream. Caution must be exercised here, as this signature can also reflect a residual noise event in the B-Field data. In this situation, careful examination of the dB/dt on-time (in-pulse) data is required to resolve the ambiguity. If the feature were strictly a noise event, it would not be present in the dB/dt off-time data stream. This would locate the response at the resistive limit, and the mid in-pulse channel (normally identified as channel 3) would reflect little but background noise, or at best a weak negative peak. If, on the other hand, the feature does indeed reflect a superconductor, then this would locate the response at the inductive limit. In this situation, channel 3 of the dB/dt stream will be a mirror image of the transmitted pulse, i.e. a large negative.

One thing to note are the data units for the B-Field data, delivered in femtoteslas (fT) and how these compare to the regular dB/dt data, delivered in pT/s (picoteslas per second). After standard processing, the resolution (mean noise envelope) of the dB/dt data is approximately 1200 – 2000 pT/s. The corresponding resolution of the B-Field data, after regular processing is approximately 2500-4000 fT or 2.5 – 4.0 picoteslas. So the amplitude ratio, based on the residual noise levels after processing, of B-Field over dB/dt is approximately 2:1. This is an important factor when trying to image or display the data.

Calculation of the Decay Constant

Calculation of the decay constant (also known as tau) is done by fitting the data from the appropriate off-time channels (mapping the decay transient) to a single exponential function of the form :

$$Y = Ae^{-t/\tau}$$

where A = the amplitude at time zero, t = time is seconds and τ is the decay constant.

A semi-log plot of this exponential function will be displayed as a straight line, the slope of which will reflect the rate of decay and therefore the strength of the conductor. A slow rate of decay, reflecting high conductance, will be represented by a high decay constant value. For the present dataset, two decay constants were calculated by fitting each the X and Z-coil response from channels 8 to 20 (mean delay times of 412 to 3038 μ sec after turn-off) of the dB/dt component to the exponential function.

As a single parameter, the decay constant provides more useful information than the amplitude data of any given single channel, as it indicates not only the peak of the response but also the relative strength of the conductor. It also allows better discrimination of conductive axes within a broad formational group of conductors. Also, unlike any quantitative value derived from the data, such as conductance or resistivity, the decay constant is the expression of a simple mathematical function which is model independent, such that it is a truer representation of the data. The only disadvantage of this parameter is that, in order to get a reliable fit of the data to the exponential function, a minimum amount of signal above the background is required to avoid introducing noise into the calculation. In essence, this means that the decay constant will effectively map features of moderate to high conductance, but weaker, more resistive features will best be defined by the apparent conductance or resistivity calculation.

Calculation of the Apparent Conductance

Both conductance (i.e. conductivity-thickness product) and resistivity values can be derived from TDEM data. However, since electromagnetic surveys, conducted for the purposes of base mineral exploration, have for their prime objective the definition of conductors, it is generally better to display the data as “conductance” as opposed to “resistivity”. Regions of high resistivity correspond to low conductive background areas, which are less significant than the resistivity lows that actually identify conductors. For this reason, preference was to provide the apparent conductance.

The apparent conductance values are derived from the full 20 channels (on-time and off-time) of the combined X and Z-coil data, fitted to a horizontal thin sheet model. The introduction of the on-time data into the calculation extends the resolution of the system at the resistive limit by approximately 2 or 3 orders of magnitude, allowing conductivities to be mapped from 10^{-5} siemens to 10^3 siemens (100,000 ohm-metres to 0.001 ohm-metre). For the present data set, the horizontal sheet model is used in fitting the resulting conductance values, stored in millisiemens.

The thickness of the layer used is infinite, as the calculated conductance is equal to the conductivity-thickness-product which is not unique. The ability to define the thickness of a conductive layer is related to the skin depth which itself is a function of the conductivity of the material and its thickness (e.g. 100 metres of 3 siemens/metre material will have the same conductance as 10 metres of 30 siemens/metre material). So, from the calculated conductance, the conductivity of a material can only be estimated if the thickness of the layer is known.

Residual errors are extracted from the data through a proprietary statistical levelling tool. This tool analyzes the background data and calculates a mean for each line of the background. The

tool then calculates the mean of all means and applies a dc shift to each line to try and bring each individual mean to the mean of all means.

The EM Anomaly Selection

EM anomalies are selected and stored in the database. An automatic routine locates all the anomaly peaks from a reference channel and fits the off-time data, above a pre-set noise background, to a vertical plate model, in order to derive the conductivity-thickness-product and the depth to the top of the conductor. The initial selection is then reviewed interactively, by an experienced interpreter, using a graphic viewing/editing tool where the anomaly selections are checked against a multi-channel profile display of the data. Corrections are made (erroneous selections deleted and missing ones added) and the selected anomalies are classified as to their possible source (surficial, bedrock or culture). The resulting anomaly selection is then checked with the magnetic signature and other derived EM parameters (decay constant and conductance) for geological significance and a final revision made. Base map information and the flight video tapes are also checked, during this process, to help in the final sorting between man-made responses and geological sources.

Discussion on filtering and gridding

The design of all filter parameters is controlled by power spectra analysis and by testing on selected portions of the data and graphically viewing the results pre- and post-filtering, to ensure that the full resolution of the geological signal is preserved while minimizing the non-geological signal.

Routinely three different gridding algorithms are used: a modified Akima spline routine for regular gridding, a linear interpolation routine for skewed data (a large amount of data at a single value), and a minimum curvature routine, usually for under-sampled data. The minimum curvature gridding is used on this project for the magnetic data to better represent small, single line features in the data which are not adequately sampled by the 200 metre line spacing. The Akima spline routine is used for the gridding of the apparent conductance, and the digital terrain model. The linear interpolation routine is used for the decay constants to accurately define the edges of the signal from the background value.

Gridding is normally done by interpolating the data at right angles to the line direction. Geological features which are orthogonal to the survey line direction will be best represented in this manner, but features which trend at an oblique angle to the line direction will often be poorly represented, appearing as broken-up segments. This situation presented itself with the magnetic data which displayed the response of numerous dykes trending at shallow angles to the flight lines. This grid is used for the map presentation of the residual magnetic field and second vertical derivative.

Fixed-wing TDEM systems exhibit an asymmetry in the response due to the system's geometry (i.e. physical separation between the transmitter loop and the receiver coils). The amount of asymmetry in the response also varies with the geometry of the conductor itself. A system lag

correction is applied during the processing to align the responses, from one survey line to the next, over narrow vertical conductors, such that these will be displayed as straight axes. However, this will leave the edges of broad flat-lying conductors displaying a line-to-line oscillation or “herringbone” pattern. This, in itself, is a useful interpretation aid, as it helps to distinguish between vertical and flat-lying conductors but as a regional mapping presentation, it presents an unappealing image. This asymmetry, associated with the edges of flat-lying conductors, can be removed by applying a de-corrugation technique directly to the gridded values. This step is often referred to as “de-herringboning”.

In the North Spirit Lake area, it was determined that the apparent conductance grids exhibited some line level noise that could not be ascribed to system asymmetry. Therefore, microlevelling was applied as an intermediate step prior to de-herringboning, and grids of the microlevelled data were prepared as well. Various microlevel filter lengths were tested, and a 15 millisiemen threshold provided the best results. It is possible that the microlevelling process removed some of the valid responses related to system asymmetry and consequently, three versions of each EM grid are provided for comparison: regular, microlevelled and de-herringboned. The de-herringboned grids are used for the map presentation.

6) MICROLEVELLING AND GSC LEVELLING OF THE MAGNETIC DATA

Microlevelling

Microlevelling is the process of removing residual flight line noise that remains after conventional levelling using control lines. It has become increasingly important as the resolution of aeromagnetic surveys has improved and the requirement of interpreting subtle geophysical anomalies has increased. The frequency-domain filtering technique known as “decorrugation” has proven inadequate in most situations, as significant geological signal might be removed along with noise. In addition, the microlevelling correction is applied to the profile data, whereas decorrugation corrects only grids. The separation of noise from geological signal, and the correction of the profiles, are the key strengths of the Paterson, Grant & Watson Limited’s (PGW) microlevelling procedure.

The PGW microlevelling technique resulted from a new application of filters used in the process of draping profile data onto a regional magnetic datum (Reford et al., 1990). It is similar to that published by Minty (1991).

Microlevelling is applied in two stages. The decorrugation stage is carried out as follows:

- Grid the flight line data to a specified cell size using the minimum curvature gridding algorithm.
- Apply a decorrugation filter in the frequency-domain, using a sixth-order high pass Butterworth filter of specified cut-off wavelength (typically four times the flight line separation), together with a directional cosine filter, so that a grid of flight line-oriented noise is generated.
- Extract the noise from the grid to a new profile channel.

At this stage, the noise grid may be examined to ensure that the flight line noise has been isolated, and to determine what parameters will be required to separate the true residual flight line noise from the high-frequency geological signal incorporated in the filtering described above.

The steps for the microlevelling stage are as follows:

- Apply an amplitude limit to clip or zero high amplitude values in the noise channel, if desired.
- Apply a low pass non-linear filter (Naudy and Dreyer, 1968), so that only the longer wavelength flight line noise remains, forming the microlevel correction.
- Subtract the microlevel correction from the original data, resulting in the final, microlevelled profile channel.

The resultant microlevelled channel can then be gridded for comparison with the original data. In addition, it is useful to examine the intermediate noise channels in profile and grid form, to verify that the desired separation of residual flight line noise and geological signal has occurred.

Microlevelling can be applied selectively to deal with noise that varies in amplitude and/or wavelength across a survey area. It can also be applied to swaths of flight lines, where more

regional level shifts are a problem due to inadequate levelling to the control lines. This can be particularly useful on older surveys where tieline data may no longer be available.

Microlevelling will not solve all problems of flight line noise. For example, positioning errors (e.g. poor lag correction) may result in some level shift that microlevelling will reduce. However, shorter wavelength anomalies will still remain mis-aligned. Line-to-line variations in survey height result in anomaly amplitude variations. Again, microlevelling will reduce long wavelength level shifts, but cannot compensate for localized amplitude changes.

In the example shown here, the data are windowed from an airborne magnetic and electromagnetic survey flown in the Matachewan area of Ontario, over typical Archean granite-greenstone terrain (Ontario Geological Survey, 1997). Standard corrections (e.g. diurnal, IGRF, conventional tieline levelling) were applied to the magnetic data. However, a considerable component of residual flight line noise remains, due for example to inadequate diurnal monitoring or tieline levelling difficulties. Figure 4 shows the decorrugation noise grid generated from the first stage. Figure 5 shows the noise channel extracted from the aforementioned grid, and the channels generated during the microlevelling stage. Figure 6 shows the residual magnetic intensity grid before and after microlevelling is applied.

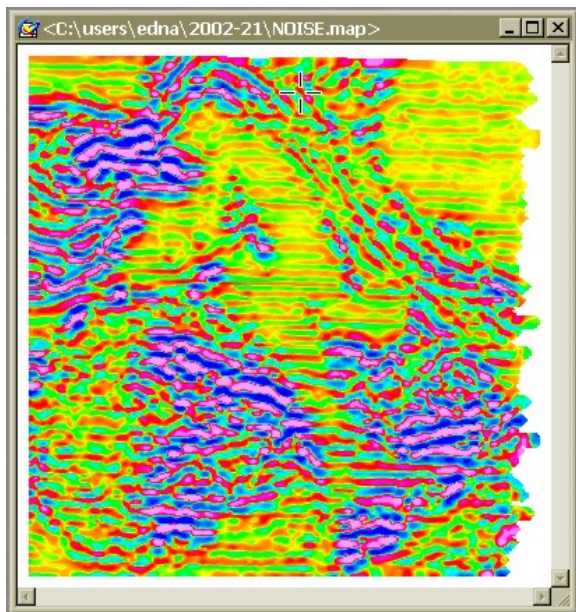


Figure 4: Decorrugation noise grid from the Matachewan microlevelling example.

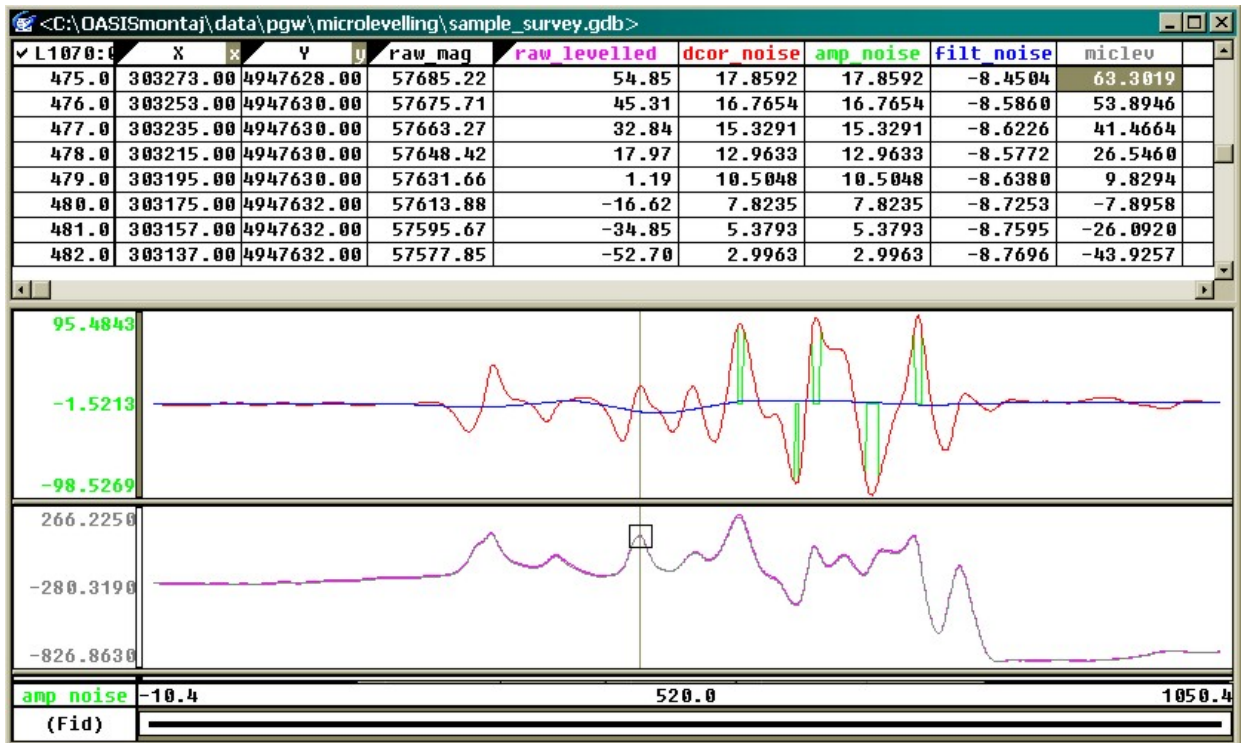


Figure 5: Data channels for microlevelling from the Matachewan microlevelling example

- Middle panel: red – decorrugated noise channel
green – noise channel after zeroing high values
blue – non-linear filtered noise channel (= microlevel correction channel)
- Lower panel: magenta – original total magnetic field
grey – microlevelled total magnetic field

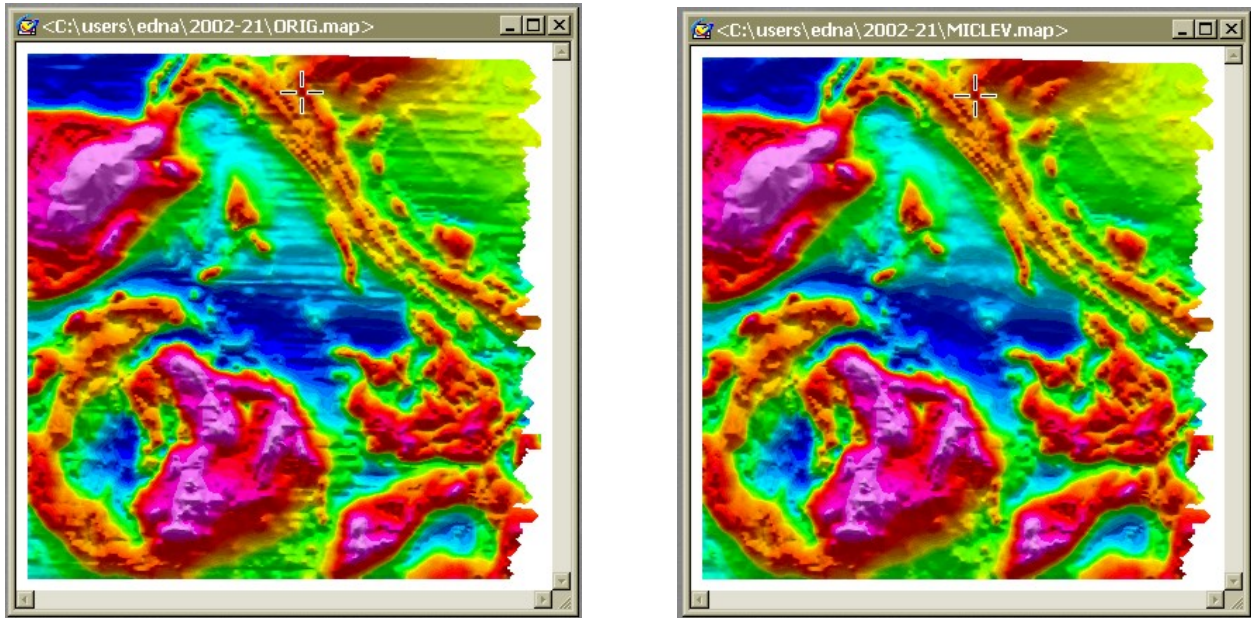


Figure 6: Total magnetic field grid, before microlevelling (left) and after microlevelling (right).

Decorrugation Parameters

Decorrugation requires a database of geophysical data, oriented along roughly parallel survey lines. Surveys with more than one line orientation should be separated into blocks of consistent line direction. The profile channel to be microlevelled should have had all standard corrections, and conventional tieline levelling, already applied. Only traverse lines should be selected for microlevelling (i.e. no tie-lines).

Flight line spacing

The nominal flight line spacing is required to design the filter parameters. If a survey contains blocks flown at different line spacings, better results will likely be obtained if these blocks are microlevelled separately. If one is attempting to remove wider level shifts, across swaths of lines, then the average width of the swath should be specified instead.

Flight line direction

The nominal flight line direction is required so that the directional filtering incorporated in the decorrugation process has the correct orientation. Survey blocks flown with different line directions should be microlevelled separately.

Grid cell size for gridding

The cell size chosen should be small enough so that the residual flight line noise represented in the grid of original data is well-defined on a survey line basis. Thus, a grid cell size of $\frac{1}{4}$ the line spacing or smaller is recommended. However, a cell size that is too small (i.e., less than $\frac{1}{10}$ the line spacing) will not improve the microlevelling results, and will increase the processing time required.

Decorrugation cut-off wavelength

This parameter defines the cut-off wavelength of the sixth-order, high-pass Butterworth filter, that is combined with a directional cosine filter (power of 0.5) oriented perpendicular to the flight line direction, to extract the residual flight line noise component from the grid of the original data. A wavelength of four times the line spacing has typically proven to produce the best results. Setting this wavelength too small will not give the filter enough width to isolate the effect of each flight line. Setting it too large will extract more geological signal than necessary.

Microlevelling Parameters

Once decorrugation has been applied, it is recommended that the decorrugation grid be reviewed and compared to the original data. This is best done by shaded relief imaging. The purpose is to:

- Ensure that the parameters chosen when decorrugation was applied have properly isolated the residual flight line noise.
- Measure the amplitudes (e.g. determine the peak-to-trough amplitude variations between the survey lines) and wavelengths (in the flight line direction) of the residual flight line noise, from the decorrugation grid.

Amplitude limit value

The amplitude limit defines the value estimated by the user as the maximum amplitude of the residual flight line noise in a survey. If the absolute value of the decorrugation noise channel exceeds the specified amplitude for a given record, then it will be clipped to that value, or zeroed, depending on the mode chosen. This is one of the techniques employed to separate residual flight line noise from geological signal. It is assumed that any responses of higher amplitude reflect geology.

The user should also consider the sources of noise for the particular survey that is being microlevelled. When considering aeromagnetic data, the noise amplitudes produced by some sources (e.g. diurnal variation) are not affected by the geological signal of an area, whereas the noise amplitudes from others (e.g. height variations) are affected by the geology, particularly where the magnetic gradients are strong.

If the user does not want to apply an amplitude limit, then a large value, exceeding the dynamic range of the decorrugation noise channel, should be specified. This dynamic range can be determined from the channel statistics.

Amplitude limit mode

There are two choices for the amplitude limit mode:

Zero mode – This will set any value in the decorrugation noise channel, whose absolute value exceeds the specified amplitude limit value, to zero prior to application of the non-linear filter. This is suited to areas where the responses exhibit steep gradients (e.g. magnetic survey over near-surface igneous and metamorphic rocks). It has the effect of dividing a simple, high amplitude response into three parts: two flanks centered on a zeroed section, allowing a shorter non-linear filter wavelength to be applied, if appropriate. It also reduces the possibility of this filter distorting a response whose wavelength is close to the filter wavelength.

Clip Mode – This will set any value in the decorrugation noise channel, whose absolute value exceeds the specified amplitude limit value, to the amplitude limit value (with appropriate sign) prior to application of the non-linear filter. This is suited to areas where the magnetic responses exhibit shallow gradients (e.g. magnetic survey over sedimentary terrain). It is also applied where the wavelengths of the residual flight line noise in the line direction are clearly much greater than those of the geological signal in the decorrugation noise grid.

Naudy filter length

The Naudy non-linear low pass filter (Naudy and Dreyer, 1968) is used due to its superior qualities for either accepting or rejecting responses beyond the specified filter length. A linear filter, in contrast, would smear an undesirable, short wavelength response into the filtered data, rather than completely remove it. It is applied to the amplitude-limited noise channel, to remove any remaining geological signal. The filter length is set to half the length of the shortest linear noise segments visible in the decorrugation noise grid. In most situations, the lengths of these noise segments will still be considerably larger than the wavelengths of geological signal. The exception occurs where there is strong signal due to geology (e.g. magnetic dykes) that strike sub-parallel with the line direction. In such cases, it is wise to choose a fairly long filter length for the first pass of microlevelling, and then shorten the filter length for any subsequent microlevelling applied only to survey lines (or parts thereof) where problems remain.

Naudy filter tolerance

This parameter sets the amplitude below which the filter will not alter the data. For microlevelling, it is recommended that this value be set quite small (e.g. 0.001 nT for magnetic data) as otherwise, the filtered noise channel may contain low amplitude, high frequency chatter that will then be introduced into the microlevelled channel when the correction is applied.

Quality control

Once the microlevelling process has been applied, it is instructive to study five parameters, both in profile and gridded form: original un-microlevelled data, decorrugated noise, amplitude-limited noise, non-linear filtered noise (i.e. microlevel correction) and microlevelled data. This will allow the user to determine if separation of residual flight line noise from geological signal is satisfactory, and whether any levelling problems remain.

Shaded relief imaging of the total magnetic field and its residual component along with first or second vertical derivatives will verify that both the residual line noise has been minimized and no new line noise has been introduced. A grid of the microlevel correction will confirm that geological signal has not been removed.

GSC Levelling

In 1989, as part of the requirements for the contract with the Ontario Geological Survey (OGS) to compile and level all existing Geological Survey of Canada (GSC) aeromagnetic data (flown prior to 1989) in Ontario, PGW developed a robust method to level the magnetic data of various base levels to a common datum provided by the GSC as 812.8 m grids. The essential theoretical aspects of the levelling methodology were fully discussed in Gupta et al. (1989), and Reford et al. (1990). The method was later applied to the remainder of the GSC data across Canada and the high-resolution AMEM surveys flown by the OGS (Ontario Geological Survey, 1996). It has since been applied to all newly acquired OGS aeromagnetic surveys.

Terminology

Master grid – refers to the 200 metre Ontario magnetic grid compiled and levelled to the 812.8 metre magnetic datum from the Geological Survey of Canada.

GSC levelling – the process of levelling profile data to a master grid, first applied to GSC data.

Intra-survey levelling or microlevelling – refers to the removal of residual line noise described earlier in this chapter; the wavelengths of the noise removed are usually shorter than tie line spacing.

Inter-survey levelling or GSC levelling – refers to the level adjustments applied to a block of data; the adjustments are the long wavelength (in the order of tens of kilometres) differences with respect to a common datum, in this case, the 200 metre Ontario master grid, which was derived from all pre-1989 GSC magnetic data and adjusted, in turn, by the 812.8 metre GSC Canada wide grid.

The GSC Levelling Methodology

The GSC levelling methodology is described below, using the Vickers survey flown for OGS as an example.

Several data processing procedures are assumed to be applied to the survey data prior to levelling, such as microlevelling, IGRF calculation and removal. The final levelled data are gridded at 1/5 of the line spacing. If a survey was flown as several distinct blocks with different flight directions, then each block is treated as an independent survey.

The steps in the GSC levelling process are as follows:

1. Create an upward continuation of the survey grid to 305m

Almost all recent surveys (1990 and later) to be compiled were flown at a nominal terrain clearance of 100 metres or less. The first step in the levelling method is to upward continue the survey grid to 305 metres, the nominal terrain clearance of the Ontario master grid (Figure 7). The grid cell size for the survey grids is set at 100 metres. Since the wavelengths of level corrections will be greater than 10 to 15 kilometres, working with 100 metre or even 200 metre grids at this stage will not affect the integrity of the levelling method. Only at the very end, when the level corrections are imported into the databases, will the level correction grids be re-gridded to 1/5 of line spacing.

The un-levelled 100 metre grid is extended by at least 2 grid cells beyond the actual survey boundary, so that, in the subsequent processing, all data points are covered.

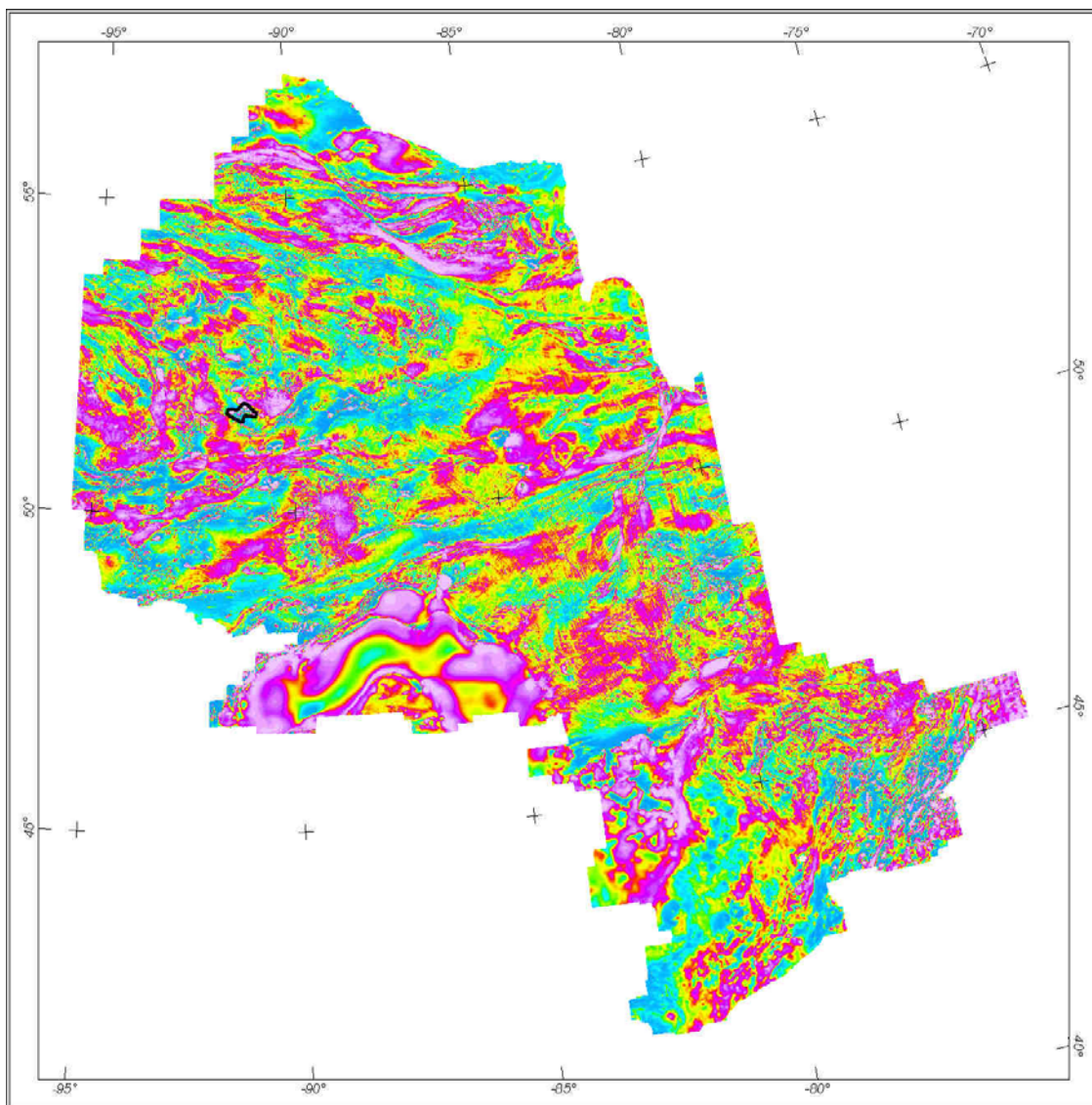


Figure 7: Ontario Master Aeromagnetic Grid (Ontario Geological Survey, 1999). The outline for the sample data set to be levelled (Vickers) is shown.

2. Create a difference grid between the survey grid and the Ontario master grid

The difference between the upward continued survey grid and the Ontario master grid, re-gridded at 100 metres, is computed (Figure 8). The short wavelengths represent the higher resolution of the survey grid. The long wavelengths represent the level difference between the two grids.

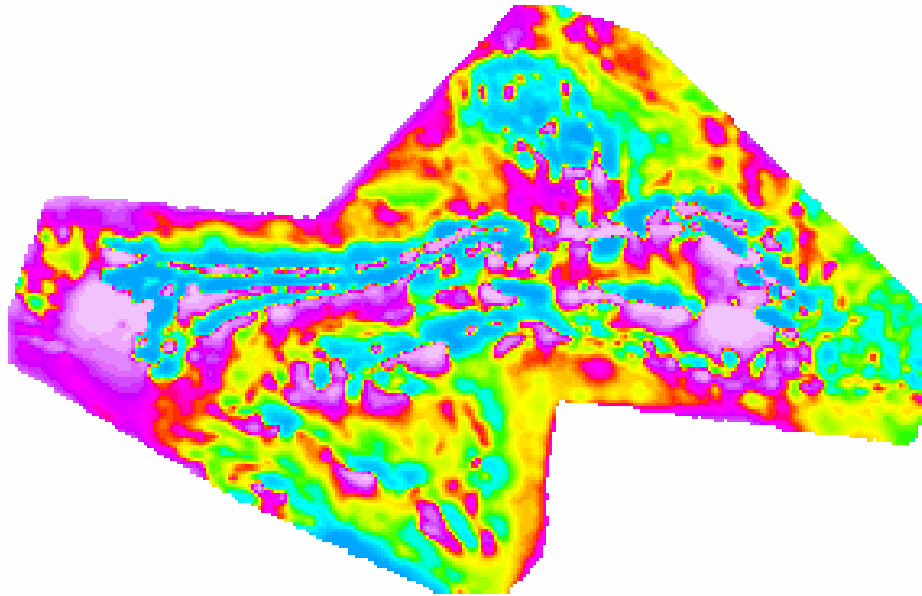


Figure 8: Difference grid (difference between survey grid and master grid), Vickers survey.

3. Rotate difference grid so that flight line direction is parallel to grid column or row, if necessary.
4. Apply the first pass of a non-linear filter (Naudy and Dreyer, 1968) of wavelength on the order of 15 to 20 kilometres along the flight line direction. Reapply the same non-linear filter across the flight line direction.
5. Apply the second pass of a non-linear filter of wavelength on the order of 2000 to 5000 metres along the flight line direction. Reapply the same non-linear filter across the flight line direction.
6. Rotate the filtered grid back to its original (true) orientation (Figure 9).

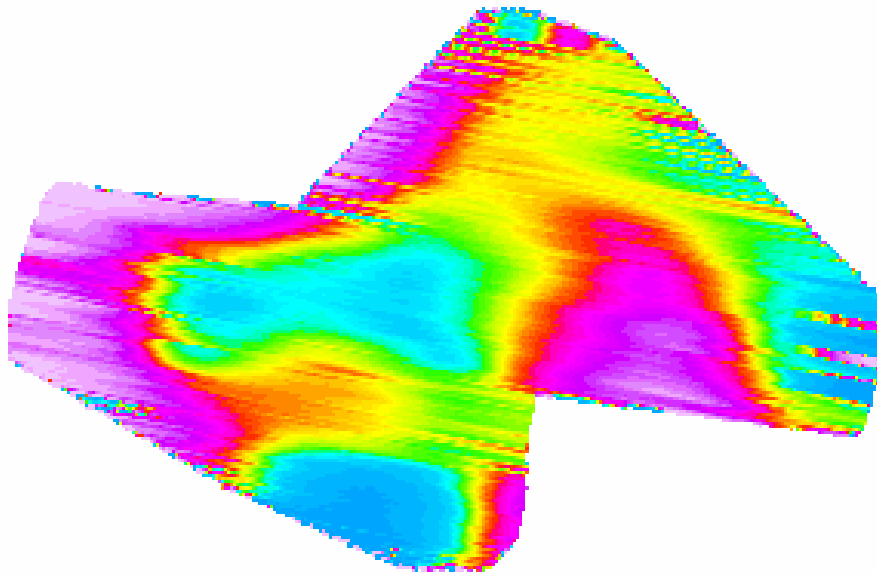


Figure 9: Difference grid after application of non-linear filtering and rotation, Vickers Survey.

7. Apply a low pass filter to the non-linear filtered grid

Streaks may remain in the non-linear filtered grid, mostly caused by edge effects. They must be removed by a frequency-domain, low pass filter with the wavelengths in the order of 25 kilometres (Figure 10).

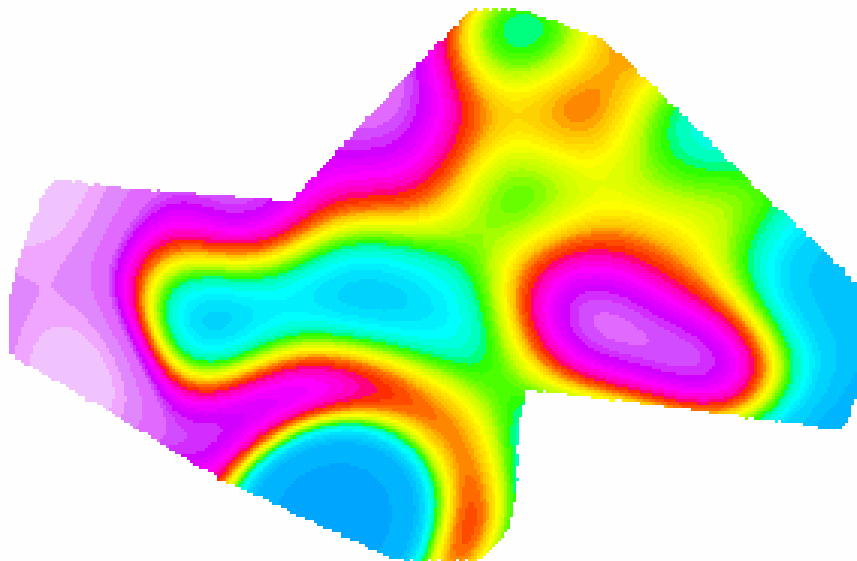


Figure 10: Level correction grid, Vickers survey.

8. Re-grid to 1/5 line spacing and import level corrections into database.

9. Subtract the level correction channel from the un-levelled channel to obtain the level corrected channel.
10. Make final grid using minimum curvature gridding algorithm with grid cell size at 1/5 of line spacing.

Total Magnetic Field and Second Vertical Derivative Grids

For most surveys the reprocessed total field magnetic grid was calculated from the final reprocessed profiles by a minimum curvature algorithm (Briggs, 1974). The accuracy standard for gridding is that the grid values fit the profile data to within 1 nT for 99.98% of the profile data points. The average gridding error is well below 0.1 nT.

Minimum curvature gridding provides the smoothest possible grid surface that also honours the profile line data. However, sometimes this can cause narrow linear anomalies cutting across flight lines to appear as a series of isolated spots.

The second vertical derivative of the total magnetic field is computed to enhance small and weak near-surface anomalies and as an aid to delineate the contacts of the lithologies having contrasting susceptibilities. The location of contacts or boundaries is usually traced by the zero contour of the second vertical derivative map.

The second vertical derivative filter incorporated an 8th-order low-pass Butterworth filter with a cut-off wavelength of 100 m (i.e. half the line spacing). The purpose of the low-pass filter is to minimize grid aliasing effects in the total magnetic field, which are emphasized by the second vertical derivative.

Survey Specific Parameters

The approach to microlevelling applied by Fugro uses different filters than those described above. The program uses two directional triangular filters, first the along line filter set to a width of 300 m (i.e. four times the sensor height, to retain the high frequency content along the lines) then an across line triangular set to a width of 400 m (i.e. twice the line spacing). The along line filter is then repeated to ensure maximum retention of the high frequencies. The main correction is applied by the across line filter then the high frequency content is added back. The threshold limits for the amplitude of the microlevelling corrections were:

- Block A (Main) – 25 nT
- Block B (North) – 10 nT.

The following GSC levelling parameters were used in the North Spirit Lake survey:

- Distance to upward continue: 230 metres
- First pass non-linear filter length: 50,000 metres
- Second pass non-linear filter length: 50,000 metres
- Low pass filter cut-off wavelength: 40,000 metres

7) FINAL PRODUCTS

The following products were delivered to MNDM:

Map products at 1:20,000

Residual magnetic field contours, plotted with flight path, Keating kimberlite coefficient anomalies and EM anomalies on a planimetric base.

Map products at 1:50,000

- Colour residual magnetic field grid with contours, plotted along with EM anomalies on a planimetric base
- Shaded colour image of the second vertical derivative of the magnetics and Keating kimberlite coefficient anomalies on a planimetric base
- Colour EM X-coil decay constant (de-herringboned) with contours and EM anomalies on a planimetric base
- Colour apparent conductance (microlevelled and de-herringboned) with contours and EM anomalies on a planimetric base

Profile databases

- EM database at 4 samples/sec in both Geosoft[®] GDB and ASCII format
- Magnetic database at 10 samples/sec in both Geosoft[®] GDB and ASCII format

EM anomaly database

EM anomaly database in both Geosoft[®] GDB and ASCII CSV format

Kimberlite coefficient database

Keating kimberlite coefficient anomaly database in both Geosoft[®] GDB and ASCII CSV format.

Data grids

Data grids, in both Geosoft[®] GRD and GXF formats, gridded from coordinates in UTM Zone 15N, NAD83 datum, of the following parameters:

- Digital elevation model
- GSC levelled magnetic field
- Second vertical derivative of the GSC levelled magnetic field
- EM X-coil decay constant (regular grid)
- EM X-coil decay constant (de-herringboned grid)
- EM Z-coil decay constant (regular grid)
- EM Z-coil decay constant (de-herringboned grid)
- Apparent conductance (regular grid)
- Apparent conductance (microlevelled grid)

- Apparent conductance (de-herringboned grid)

GeoTIFF images of the total of the 1:50,000 map sheets

- Colour residual magnetics on a planimetric base
- Colour shaded relief of the second vertical derivative of the magnetic field on a planimetric base
- Colour de-herringboned EM X-coil decay constant on a planimetric base
- Colour de-herringboned apparent conductance on a planimetric base

DXF vector files of the entire survey block

- Flight path
- EM anomaly locations
- Keating kimberlite coefficient anomalies
- Residual magnetic field contours
- De-herringboned EM X-coil decay constant contours
- De-herringboned apparent conductance contours

Halfwave files

These are compressed ASCII files, covering one flight of data per file. These files contain the 384 points of the TDEM waveform, stacked to 4 Hz sampling, for the four components:

- T (transmitted electromagnetic field)
- X (X-component of the secondary electromagnetic field)
- Y (Y-component of the secondary electromagnetic field)
- Z (Z-component of the secondary electromagnetic field)

Note that for the 90 Hz transmitter base frequency, the waveform is only defined by the first 128 points. The remaining 256 points, in this case, are simply filled with zeroes.

Waveform parameter table files

These are the TDEM reference waveform files delivered as standard ASCII text files, one for each survey flight. These files provide information on the system geometry, the window (channel) positions, the conversion factors and the waveform itself.

Project report

Provided in both Microsoft® Word and Adobe® PDF formats.

Raw Streamed Files

These are the raw uncompressed binary files directly from the Analogue to Digital converter on the aircraft. These are provided with a binary to ASCII converter as well as a technical descriptor of the output. Refer to “Raw_streamed_format_newrec.doc” in the raw streamed directory of the data products for more information.

Flight Videos

The digitally recorded video from each survey flight are provided in a compressed binary format.

8) QUALITY ASSURANCE AND QUALITY CONTROL

Quality assurance and quality control (QA/QC) were undertaken by Fugro Airborne Surveys, by PGW (FNGMI Geophysicist), and by MNM. Stringent QA/QC is emphasized throughout the project so that the optimal geological signal is measured, archived and presented.

Survey Contractor

Important checks are required during the data acquisition stage to ensure that the data quality is kept within the survey specifications. The following lists in detail the standard data quality checks that were performed during the course of the survey.

Daily quality control

Navigation data

- The differentially corrected GPS flight track is recovered and matched against the theoretical flight path to ensure that any deviations are within the specifications (i.e. deviations not greater than 50 m from the nominal line spacing over a 2 km distance).
- All altimeter data (radar, barometric and GPS elevation) are checked for consistency and deviations in terrain clearance were monitored closely. The survey is flown in a smooth drape fashion maintaining a nominal terrain clearance of 120 metres, whenever possible. Altitude corrections are done in a smoothly controlled manner, rather than forcing the aircraft to return to the nominal altitude, to avoid excessive motion of the towed-bird which would impact on the quality of the data. A digital elevation trace, calculated from the radar altimeter and the GPS elevation values, is also generated to further control the quality of the altimeter data.
- The synchronicity of the GPS time and the acquired time of the geophysical data is checked by matching the recorded time fields.
- A final check on the navigation data is done by computing the point-to-point speed from the corrected UTM X and Y values. The computed values should be free of erratic behaviour, showing a nominal ground speed of 65 m/s with point-to-point variations not exceeding +/- 10 m/s except where flying conditions dictate otherwise.

Magnetometer data

- The diurnal variation is examined for any deviations that exceed the specified 3 nT peak-to-peak over a chord equivalent to approximately 60 seconds. Data was re-flown when this condition was exceeded, with any re-flown line segment crossing a minimum of two control lines. A further quality control done on the diurnal variation is to examine the data for any man-made disturbances. When noted, these artefacts are graphically removed by a polynomial interpolation so that they are not introduced

into the final data when the diurnal values are subtracted from the recorded airborne data.

- The integrity of the airborne magnetometer data is checked through statistical analysis and graphically viewed in profile form, to ensure that there are no gaps and that the noise specifications are met.
- A fourth difference editing routine is applied to the raw data to locate and correct any small steps and/or spikes in the data.
- Any effects of filtering applied to the data are examined by displaying, in profile form, the final processed results against the original raw data, via a graphic screen. This is done to ensure that any noise filtering applied has not compromised the resolution of the geological signal.
- Ongoing gridding and imaging of the data is also done to control the overall quality of the magnetic data.

Electromagnetic data

- The high altitude calibration sequences, recorded pre- and post-flight, are closely examined. These background data segments, which are free of ground conductive response, are checked to ensure that the baseline positions for each channel are good, that the noise levels are within specified limits and that the system has been well compensated for excessive motion of the towed-bird.
- The reference waveform, collected during the calibration sequence and used for the compensation of the primary field, is closely examined for consistency from flight to flight. Diagnostic parameters, such as the peak voltages for each coil set and the transmitter current are noted and entered in the daily processing log for future reference.
- All recorded EM channels are examined and adjusted for system drift. This is done by graphically displaying each channel data in profile for the entire flight as a continuous segment and checking the high altitude background segments and local minima against a zero baseline value. This check also provides a good overall view of the response from each channel for any unusual behaviour.
- Level of spheric activity is assessed during the processing, through a decay analysis. The percentage of bad decays detected that are not associated with power lines, are tabulated and reported. Under normal conditions, this is kept to 1% or less.
- The “streamed” data is checked for continuity and its integrity assessed by statistical analysis. A viewing tool is also used to display the transient/waveform response from each of the four measured components: Tx, Rx, Ry and Rz.

- After processing, the final results are displayed in profile form, via a graphic screen and compared with the raw data, to ensure that the data has not been over filtered. A multi-channel profile display of the data, at this stage, also provides a visual check on the character of the decay information. This is followed by the calculation of the decay constant itself, which is gridded and imaged on an on-going basis throughout the survey, to further control the quality of the electromagnetic data.

Near-final field products

Near-final products of the profile and gridded navigation, magnetic and electromagnetic data were made available to the FNGMI Geophysicist during visits to the survey site, for review and approval, prior to demobilization.

Quality control in the office

Review of field processing of magnetic and electromagnetic data

The general results of the field processing are reviewed in the profile database by producing a multi-channel stacked display of the data (raw and processed) for every line, using a graphic viewing tool. The magnetic and altimeter data are checked for spikes and residual noise. The electromagnetic channel data is checked for baseline positions, decay character and the effect of filtering.

Review of levelling of magnetics

The results of the field levelling of the magnetics are reviewed, using imaging and shadowing techniques. Any residual errors noted are corrected and the final micro-levelling re-applied to the profile data.

Creation of second vertical derivative

The second vertical derivative is created from the final gridded values of the total field magnetic data and checked for any residual errors using imaging and shadowing techniques.

Creation of final electromagnetic grids

EM grids of the X and Z-coil decay constant (τ) and the apparent conductance values are created, reviewed for residual drift/levelling errors and the necessary corrections applied. At this stage, the option of using either the regular dB/dt coil data or the B-Field components, to generate the required parameter grids, is reviewed to ensure the best definition of the targets sought. Necessary material is provided to the FNGMI Geophysicist for this evaluation.

Correction of electromagnetic grids for asymmetry

The selected EM grids are corrected for asymmetry (de-herringboned) and checked against the original grids to ensure that there is no loss or misrepresentation of geological features.

Electromagnetic anomaly selection

The automated EM anomaly selection is reviewed interactively against the profile data, via a graphic display tool and edited to ensure that all valid anomalies are represented in the database. The final selection is then checked against the base maps (and in-flight videos, as required) to properly separate and label man-made responses from geological sources.

Interim products

Archive files containing the raw and processed profile data, the EM anomaly database and the final gridded parameters are provided to the FNGMI Geophysicist for review and approval.

Creation of 1:20,000 and 1:50,000 maps

After approval of the interim data, the 1:20,000 and 1:50,000 maps are created and verified for registration, labelling, dropping weights, general surround information, etc. The hard copy and corresponding digital files are provided to the FNGMI Data Manager for review and approval.

FNGMI Geophysicist

The FNGMI Geophysicist conducted on-site inspections during data acquisition, focusing initially on the data acquisition procedures, base station monitoring and instrument calibration. As data was collected, it was reviewed for adherence to the survey specifications and completeness. Any problems encountered during data acquisition were discussed and resolved.

The QA/QC checks included the following:

Navigation data

- appropriate location of the GPS base station
- flight line and control line separations are maintained, and deviations along lines are minimized
- verify synchronicity of GPS navigation and flight video
- all boundary control lines are properly located
- terrain clearance specifications are maintained
- aircraft speed remained within the satisfactory range
- area flown covers the entire specified survey area
- differentially-corrected GPS data does not suffer from satellite-induced shifts or dropouts
- GPS height and radar/laser altimeter data are able to produce an image-quality DEM
- GPS and geophysical data acquisition systems are properly synchronized
- GPS data are adequately sampled.

Magnetic data

- appropriate location of the magnetic base station, and adequate sampling of the diurnal variations
- heading error and lag tests are satisfactory

- magnetometer noise levels are within specifications
- magnetic diurnal variations remain within specifications
- magnetometer drift is minimal once diurnal and IGRF corrections are applied
- spikes and/or drop-outs are minimal to non-existent in the raw data
- filtering of the profile data is minimal to non-existent
- in-field levelling produces image-quality grids of the total magnetic field and higher-order products (e.g. second vertical derivative of the magnetic field).

Time-domain electromagnetic data

- selected receiver coil orientations, base frequency, primary field waveform and secondary field sampling are appropriate for the local geology
- raw "streaming" data are recorded and archived
- data behaves consistently between channels (i.e. consistent signal decay)
- noise levels are within specifications, and system noise is minimized
- bird swing and orientation noise is not evident
- spherics and other spikes are minimal (after editing)
- cultural (60 Hz) noise is not excessive
- regular tests are conducted to monitor the reference waveform and system drift, and to ensure proper zero levels
- filtering of the profile data is minimal
- in-field processing produces image-quality data of apparent conductivity and decay constant (τ).

The FNGMI Geophysicist reviewed interim and final digital and map products throughout the data compilation phase, to ensure that noise was minimized and that the products adhered to the FNGMI specifications. This typically resulted in several iterations before all digital products were considered satisfactory. Considerable effort was devoted to specifying the data formats and verifying that the data adhered to these formats.

MNDM

MNDM prepared all of the base map and map surround information required for the digital and hard copy maps. This ensured consistency and completeness for all of the FNGMI geophysical map products. The base map was constructed from digital files of the 1:50,000 NTS map series.

MNDM worked with the FNGMI Geophysicist to ensure that the digital files adhered to the specified ASCII and binary file formats, that the file names and channel names were consistent, and that all required data were delivered on schedule. The map products were carefully reviewed in digital and hard copy form to ensure legibility and completeness.

MNDM provided QA/QC of the magnetic profile and gridded data prepared by PGW as part of the GSC levelling process.

REFERENCES

- Briggs, Ian, 1974, Machine contouring using minimum curvature, *Geophysics*, v.39, pp.39-48.
- Gupta, V., Paterson, N., Reford, S., Kwan, K., Hatch, D., and Macleod, I., 1989, Single master aeromagnetic grid and magnetic colour maps for the province of Ontario, in Summary of field work and other activities 1989, Ontario Geological Survey Miscellaneous Paper 146, pp.244-250.
- Gupta, V. and Ramani, N., 1982, Optimum second vertical derivatives in geological mapping and mineral exploration, *Geophysics*, v.47, pp. 1706-1715.
- Gupta, V., Rudd, J. and Reford, S., 1998, Reprocessing of thirty-two airborne electromagnetic surveys in Ontario, Canada: Experience and recommendations, 68th Annual Meeting of the Society of Exploration Geophysicists, Extended Technical Abstracts, p.2032-2035.
- Keating, P.B., 1995, A simple technique to identify magnetic anomalies due to kimberlite pipes, *Exploration and Mining Geology*, vol. 4, no. 2, p. 121-125.
- Minty, B. R. S., 1991, Simple micro-levelling for aeromagnetic data, *Exploration Geophysics*, v. 22, pp. 591-592.
- Naudy, H. and Dreyer, H., 1968, Essai de filtrage nonlinéaire appliqué aux profils aeromagnétiques, *Geophysical Prospecting*, v. 16, pp.171-178.
- Ontario Geological Survey, 1996, Ontario airborne magnetic and electromagnetic surveys, processed data and derived products: Archean and Proterozoic “greenstone” belts – Matachewan Area, ERLIS Data Set 1014.
- Ontario Geological Survey 2002. Ontario airborne geophysical surveys, magnetic and electromagnetic data, Vickers area; Ontario Geological Survey, Geophysical Data Set 1106rev.
- Ontario Geological Survey, 1999, Single master gravity and aeromagnetic data for Ontario, Geophysical Data Set 1036.
- Palacky, G.J. and West, G.F. 1973, Quantitative interpretation of INPUT AEM measurements, *Geophysics*, v.38, p. 1145-1158.
- Reford, S.W., Gupta, V.K., Paterson, N.R., Kwan, K.C.H., and Macleod, I.N., 1990, Ontario master aeromagnetic grid: A blueprint for detailed compilation of magnetic data on a regional scale, in Expanded Abstracts, Society of Exploration Geophysicists, 60th Annual International Meeting, San Francisco, v.1., pp.617-619.
- Smith, R.S. and Annan, A.P. 1997. Advances in airborne time-domain EM technology, in Proceedings of Exploration 97: Fourth Decennial Conference on Mineral Exploration, p. 497-504.

Smith, R.S. and Annan, A.P. 1998, The use of B-Field measurements in an airborne time-domain system, Part I: Benefits of B-Field versus dB/dt data, *Exploration Geophysics*, v.29, p. 24-29.

Smith, R.S. and Keating, P.B. 1996, The usefulness of multicomponent time-domain airborne electromagnetic measurements, *Geophysics*, v.61, p. 74-81.

Wolfgram, P. and Thomson, S. 1998, The use of B-Field measurements in an airborne time-domain system, Part II: Examples in conductive regimes, *Exploration Geophysics*, v.29, p. 225-229.

APPENDIX A TESTING AND CALIBRATION

Pre-survey Calibrations

Reid-Mahaffy Airborne Geophysical Test Site Survey

The *Reid-Mahaffy Airborne Geophysical Test Site Survey*, representing approximately 155 km of flying, was flown along the coordinates provided by MNDM. This included one line re-flown at several different elevations to provide a height attenuation calibration, and twice in each direction to verify repeatability and determine the effects of system asymmetry. This test was done to demonstrate the general functionality of all on-board systems (navigation, altimetry, magnetics and electromagnetics) and provide a comparison between different systems. Data from this test was made available to the FNGMI Geophysicist upon start-up of the program. These data were also used to generate a full suite of sample products, which were made available for review.

Readers are referred to the following publication for details on the test site:

Ontario Geological Survey 2000. Airborne magnetic and electromagnetic surveys, Reid-Mahaffy Airborne Geophysical Test Site Survey; Ontario Geological Survey, Miscellaneous Release – Data 55 (MRD-55).

Magnetometer and GPS Cloverleaf

A calibration site, selected to offer a good visual reference and a low magnetic gradient, was used to verify the heading errors of the magnetometer (basic cloverleaf test) and to verify the synchronicity between the GPS navigation and the video as well as the final accuracy of the GPS differentially corrected positions. Results of these tests were reviewed during the first field inspection by the FNGMI Geophysicist. The tests were repeated for demobilization.

Magnetometer cloverleaf test

Flown in Red Lake, ON, on November 11th, 2006 – pre survey

Line	Direction	Fiducial	Radar (m)	Diurnal (nT)	Air mag (nT)	Mag diff. (nT)
1	N	75154.6	374.17	58332.81	58344.27	-11.46
2	S	74996.8	370.02	58333.98	58346.16	-12.18
3	E	76224.2	377.41	58334.11	58346.38	-12.27
4	W	76056.2	373.4	58333.48	58345.72	-12.24

Average East-West difference = 0.70 nT

Average North-South difference = -0.70 nT

Average E-W and N-S difference = 0.15 nT

Flown in Red Lake, ON, on January 28th, 2007 – post survey

Line	Direction	Fiducial	Radar (m)	Diurnal (nT)	Air mag (nT)	Mag diff. (nT)
1	N	65161.4	657.51	58380.83	58401.45	-20.62
2	S	65393.3	655.01	58377.25	58395.67	-18.42
3	E	67092.8	655.85	58369.65	58388.44	-18.79
4	W	66861.9	656.11	58371.73	58390.77	-19.04

Average East-West difference = 0.29 nT
 Average North-South difference = -2.01 nT
 Average E-W and N-S difference = 0.33 nT

GPS lag and accuracy check

Flown in Red Lake, ON, on October 27th, 2006 – pre survey

Location (WGS84)... Lat 48° 34' 19" N
 Long 81° 22' 12" W

Resolution : 1 second = 31 m in Northing
 21 m in Easting

Line	Direction	Video	VOR offset
1	N	74939	2 m to W
2	S	75032.3	2 m to E
3	E	74305.5	5 m to N
4	W	74184.1	3 m to N

GPS lag = 0.3 second

Error box = 5 x 12 metres

Flown in Red Lake, ON, on January 28th, 2007 – post survey

Location (WGS84)... Lat 51° 04' 17" N
 Long 93° 45' 43" W

Resolution : 1 second = 31 m in Northing
 21 m in Easting

Line	Direction	Video	VOR offset
1	N	72928.6	11 m to W
2	S	73058	8 m to W
3	E	72392.4	34 m to N
4	W	72490.4	12 m to N

GPS lag = 0.33 second

Error box = 5 x 12 metres

Magnetometer and TDEM Lag Check

The system lag for the magnetometer and electromagnetic system was verified by flying several passes, in opposite directions, over a recognizable feature on the ground giving a sharp magnetic and electromagnetic response. Results of this test were made available to the FNGMI Geophysicist for the first field inspection.

Measured instrument lags were:

- Magnetometer reading lag of 3.6 seconds or 36 recording samples (10 Hz sampling)
- TDEM reading lag of 4.49 seconds or 18 recording samples (4 Hz sampling)

Pre and Post Survey Calibrations

Altimeter calibration

The accuracy and the relationship between the radar altimeter, the barometric altimeter and the GPS elevation values were verified, pre-survey, by flying a series of passes at designated altitudes over the Ottawa River.

Flown over Nighthawk Lake, on October 27th, 2006, elevation ~ 900 feet a.s.l. – pre survey

Nominal (ft)	Radar (ft)	Baro-Elev. (ft)	GPS(z)-Elev. (ft)
300	297.91	284.15	313.71
350	353.69	356.69	369.58
400	397.17	410.69	411.48
450	457.01	474.38	469.49
500	520.96	534.42	531.50
600	626.90	632.75	628.16
800	857.16	873.22	849.99

Linear regression analysis $y = a + bx$

1. Radar (x) vs. Baro (y) (minus terrain elevation)..... $1.0167x - 4.45$ ft
2. Baro (x) vs. GPS - Z (y) (both corrected for terrain)..... $0.937x + 93.801$ ft

Flown over Trout Lake, on January 28th, 2007, elevation ~ 1290 feet a.s.l. – post survey

Nominal (ft)	Radar (ft)	Baro-Elev. (ft)	GPS(z)-Elev. (ft)
300	289.94	265.92	305.88
350	344.93	364.61	359.79
400	388.54	394.70	399.62
450	446.45	448.11	458.67
500	522.34	541.65	534.24

600	576.73	572.36	582.50
800	795.71	811.91	797.37

Linear regression analysis $y = a + bx$

1. Radar (x) vs. Baro (y) (minus terrain elevation)..... $1.0388x - 13.699$ ft
2. Baro (x) vs. GPS - Z (y) (both corrected for terrain)..... $0.9298x + 130.19$ ft

Daily Calibrations

Barometric altimeter drift check

The drift in the barometric altimeter and the general accuracy of the GPS elevation values were monitored daily by setting the barometric altimeter to the runway elevation prior to take-off on each flight and noting the readings upon landing. These values were recorded in the flight log.

Pre and post-flight TDEM calibration

TDEM systems must be compensated to remove all effects of the primary field on the received secondary signal. This primarily affects the on-time channels and the early off-time channels, close to the turn-off of the pulse. This compensation is done at altitude, sufficiently high to avoid contaminating the signal with ground conductive response. System backgrounds for all channels are collected and stacked over time to provide a statistically valid reference waveform for all components (Tx, Rx, Ry and Rz). This reference waveform is then used to subtract the effects of the primary field on the received signal. Changes in the current waveform, which take place during the survey, are used to deconvolve the X,Y and Z components and remove distortion from nominal waveform to first order. Following the compensation, the aircraft is also put through a series of pitches and rolls, while still at altitude, to verify the effectiveness of the compensation during excessive motion of the receiver bird, triggered by the aircraft manoeuvres. This test is performed at the start of every flight and repeated at the end of the flight and is considered an integral part of the data. The reference waveform is also stored digitally and delivered as part of the final data.

APPENDIX B PROFILE ARCHIVE DEFINITION

Survey 1056 was carried out using the time-domain GEOTEM[®] 1000 electromagnetic and magnetic system mounted on a fixed wing platform. A transmitter base frequency of 90 Hz was used.

Data File Layout

The files for the North Spirit Lake Geophysical Survey 1056 are archived on DVD and sold as 2 separate products, as outlined below:

Type of data	Mag/EM	EM
Format	Grid/Vector and Profile data (DVD-R)	Halfwave data (DVD-R)
ASCII and Geosoft [®] Binary	1056a	1056b

The content of the ASCII and Geosoft[®] binary file types are identical. They are provided in both forms to suit the user's available software. The survey data is divided as follows:

DVD - 1056a

- ASCII (GXF) grids
 - total (residual) field magnetics
 - second vertical derivative of the total field magnetics
 - apparent conductance (initial, microlevelled and de-herringboned)
 - X-coil decay constant (initial and de-herringboned)
 - Z-coil decay constant (initial and de-herringboned)
 - digital elevation model
- EM anomaly database (ASCII CSV format)
- Keating correlation (kimberlite) database (ASCII CSV format)
- DXF files of entire survey block for:
 - flight path
 - EM anomalies
 - Keating correlation (kimberlite) anomalies
 - total field magnetic contours
 - X-coil decay constant (tau) contours
 - apparent conductance contours
- GEOTIFF images (250 dpi) of the entire survey block
 - colour total field magnetics with base map
 - colour shaded relief of second vertical derivative with base map
 - colour X-coil decay constant with base map
 - colour apparent conductance with base map
- Geosoft[®] binary (GRD) grids
 - Total (residual) field magnetics
 - second vertical derivative of the total field magnetics

- apparent conductance (initial, microlevelled and de-herringboned)
- X-coil decay constant (initial and de-herringboned)
- Z-coil decay constant (initial and de-herringboned)
- digital elevation model
- EM anomaly database (Geosoft® GDB format)
- Keating correlation (kimberlite) database (Geosoft® GDB format)
- DXF files of entire survey block for:
 - flight path
 - EM anomalies
 - Keating correlation (kimberlite) anomalies
 - total field magnetic contours
 - X-coil decay constant (tau) contours
 - apparent conductance contours

ASCII Profile data

- Profile database of magnetic data (10 Hz sampling) in ASCII (XYZ) format (Main block)
- Profile database of magnetic data (10 Hz sampling) in ASCII (XYZ) format (North block)
- Profile database of electromagnetic data (4 Hz sampling) in ASCII (XYZ) format (Main block)
- Profile database of electromagnetic data (4 Hz sampling) in ASCII (XYZ) format (North block)

Binary Profile data

- Profile database of magnetic data (10 Hz sampling) in Geosoft® GDB format (Main block)
- Profile database of magnetic data (10 Hz sampling) in Geosoft® GDB format (North block)
- Parameter table files (PTAxxx.OUT) for each flight
- Survey report (Microsoft® Word and Adobe® PDF formats)

DVD – 1056b

- Streamed halfwave electromagnetic data in WinZip®-compressed ASCII (TXT) format
- Parameter table files (PTAxxx.OUT) for each flight
- Vector files (DXF format) illustrating the flight path and flight line numbers
- Survey report (Microsoft® Word and Adobe® PDF formats)
- Readme file (Microsoft® Word and Adobe® PDF formats) describing the halfwave data structure

Coordinate Systems

The profile, electromagnetic anomaly and Keating coefficient data are provided in two coordinate systems:

- Universal Transverse Mercator (UTM) projection, Zone 15N, NAD83 datum, Canada local datum
- Latitude/longitude coordinates, NAD83 datum, Canada local datum

The gridded data are provided in one UTM coordinate system:

- Universal Transverse Mercator (UTM) projection, Zone 15N, NAD83 datum, Canada local datum

Line Numbering

The line numbering convention for survey 1056 is as follows:

Line numbers are 5 digits with the last digit indicating part or revision number
i.e. Line 10010 is the first line of the survey followed by line 10020; should line 10010 be in two parts the first is 10010 and the second is 10011

The same convention is used for the labelling of the control lines.

Main Block is covered by lines 10010 to 13910 and control lines 18010 to 18330.
North Block is covered by lines 20010 to 20790 and control lines 28010 to 28130.

Profile Data

The profile data are provided in two formats, one ASCII and one binary:

ASCII

- ASCII XYZ file of electromagnetic data, sampled at 4 Hz as two files, one for each block
 - FNNS1EM.XYZ (Main Block)
 - FNNS2EM.XYZ (North Block)
- ASCII XYZ file of magnetic data, sampled at 10 Hz as two files, one for each block
 - FNNS1MAG.XYZ (Main Block)
 - FNNS2MAG.XYZ (North Block)

Binary

- Geosoft[®] OASIS montaj binary database file (no compression) of electromagnetic data, sampled at 4 Hz as two files, one for each block
 - FNNS1EM.gdb (Main Block)
 - FNNS2EM.gdb (North Block)
- Geosoft[®] OASIS montaj binary database file (no compression) of magnetic data, sampled at 10 Hz as two files, one for each block

- FNNS1MAG.gdb (Main Block)
- FNNS2MAG.gdb (North Block)

The contents of the FNNS1EM.xyz/gdb and FNNS2EM.xyz/gdb are summarized as follows:

Channel Name	Description	Units
gps_z_final	differentially corrected GPS Z using NAD83 datum	metres above sea level
x_nad83	easting in UTM co-ordinates using NAD83 datum	metres
y_nad83	northing in UTM co-ordinates using NAD83 datum	metres
long_nad83	longitude using NAD83 datum	decimal-degrees
lat_nad83	latitude using NAD83 datum	decimal-degrees
radar_final	corrected radar altimeter	metres above terrain
baro_final	corrected barometric altimeter	metres above sea level
dem	digital elevation model	metres above sea level
fiducial	fiducial	seconds
flight	flight number	
line_number	full flightline number	
time_utc	UTC time	seconds
time_local	local time (Central Standard Time)	seconds after midnight
date	local date	YYYYMMDD
mag_final	micro-levelled magnetic field	nanoteslas
height_em	electromagnetic receiver height	metres above terrain
em_x_raw_on	raw (stacked) dB/dt, X-component, on-time	picoteslas per second
em_x_raw_off	raw (stacked) dB/dt, X-component, off-time	picoteslas per second
em_y_raw_on	raw (stacked) dB/dt, Y-component, on-time	picoteslas per second
em_y_raw_off	raw (stacked) dB/dt, Y-component, off-time	picoteslas per second
em_z_raw_on	raw (stacked) dB/dt, Z-component, on-time	picoteslas per second
em_z_raw_off	raw (stacked) dB/dt, Z-component, off-time	picoteslas per second
em_x_drift_on	drift-corrected dB/dt, X-component, on-time	picoteslas per second
em_x_drift_off	drift-corrected dB/dt, X-component, off-time	picoteslas per second
em_y_drift_on	drift-corrected dB/dt, Y-component, on-time	picoteslas per second
em_y_drift_off	drift-corrected dB/dt, Y-component, off-time	picoteslas per second
em_z_drift_on	drift-corrected dB/dt, Z-component, on-time	picoteslas per second
em_z_drift_off	drift-corrected dB/dt, Z-component, off-time	picoteslas per second
em_x_final_on	filtered dB/dt, X-component, on-time	picoteslas per second
em_x_final_off	filtered dB/dt, X-component, off-time	picoteslas per second
em_y_final_on	filtered dB/dt, Y-component, on-time	picoteslas per second
em_y_final_off	filtered dB/dt, Y-component, off-time	picoteslas per second
em_z_final_on	filtered dB/dt, Z-component, on-time	picoteslas per second
em_z_final_off	filtered dB/dt, Z-component, off-time	picoteslas per second
em_bx_raw_on	raw (stacked) B-field, X-component, on-time	femtoteslas
em_bx_raw_off	raw (stacked) B-field, X-component, off-time	femtoteslas
em_by_raw_on	raw (stacked) B-field, Y-component, on-time	femtoteslas
em_by_raw_off	raw (stacked) B-field, Y-component, off-time	femtoteslas
em_bz_raw_on	raw (stacked) B-field, Z-component, on-time	femtoteslas
em_bz_raw_off	raw (stacked) B-field, Z-component, off-time	femtoteslas
em_bx_drift_on	drift-corrected B-field, X-component, on-time	femtoteslas
em_bx_drift_off	drift-corrected B-field, X-component, off-time	femtoteslas
em_by_drift_on	drift-corrected B-field, Y-component, on-time	femtoteslas

em_by_drift_off	drift-corrected B-field, Y-component, off-time	femtoteslas
em_bz_drift_on	drift-corrected B-field, Z-component, on-time	femtoteslas
em_bz_drift_off	drift-corrected B-field, Z-component, off-time	femtoteslas
em_bx_final_on	filtered B-field, X-component, on-time	femtoteslas
em_bx_final_off	filtered B-field, X-component, off-time	femtoteslas
em_by_final_on	filtered B-field, Y-component, on-time	femtoteslas
em_by_final_off	filtered B-field, Y-component, off-time	femtoteslas
em_bz_final_on	filtered B-field, Z-component, on-time	femtoteslas
em_bz_final_off	filtered B-field, Z-component, off-time	femtoteslas
power	60 Hz power line monitor	microvolts
primary	electromagnetic primary field	parts per million
earth	earth field	parts per million
pitch	transmitter attitude – pitch	degrees
roll	transmitter attitude – roll	degrees
tau_x	decay constant (tau) for X-component	microseconds
tau_z	decay constant (tau) for Z-component	microseconds
conductance	apparent conductance	millisiemens

In the XYZ files, the electromagnetic channel data are provided in individual channels with numerical indices (e.g. em_x_final_on[0] to em_x_final_on[4], and em_x_final_off[0] to em_x_final_off[14]). In the GDB files, the electromagnetic channel data are provided in array channels with 5 elements (on-time) or 15 elements (off-time).

The contents of FNNS1MAG.xyz/gdb and FNNS2MAG.xyz/gdb are summarized as follows:

Channel Name	Description	Units
gps_x_raw	raw GPS X	metres
gps_y_raw	raw GPS Y	metres
gps_z_raw	raw GPS Z	metres
gps_base_x	GPS base station X	decimal-degrees
gps_base_y	GPS base station Y	decimal-degrees
gps_base_z	GPS base station Z	metres
gps_z_final	differentially corrected GPS Z using NAD83 datum	metres above sea level
x_nad83	easting in UTM co-ordinates using NAD83 datum	metres
y_nad83	northing in UTM co-ordinates using NAD83 datum	metres
lon_nad83	longitude using NAD83 datum	decimal-degrees
lat_nad83	latitude using NAD83 datum	decimal-degrees
radar_raw	raw radar altimeter	metres above terrain
radar_final	corrected radar altimeter	metres above terrain
baro_raw	raw barometric altimeter	metres above sea level
baro_final	corrected barometric altimeter	metres above sea level
dem	digital elevation model	metres above sea level
fiducial	fiducial	seconds
flight	flight number	
line_number	Full flightline number	
time_utc	UTC time	seconds
time_local	local time (Central Standard Time)	seconds after midnight
date	local date	YYYYMMDD
height_mag	magnetometer height	metres above terrain
mag_base_raw	raw magnetic base station data	nanoteslas
mag_base_final	corrected magnetic base station data	nanoteslas
mag_raw	raw magnetic field	nanoteslas
mag_edit	edited magnetic field	nanoteslas
mag_diurn	diurnally-corrected magnetic field	nanoteslas
igrf	local IGRF field	nanoteslas
mag_igrf	IGRF-corrected magnetic field	nanoteslas
mag_lev	levelled magnetic field	nanoteslas
mag_final	micro-levelled magnetic field	nanoteslas
mag_gsclevel	GSC levelled magnetic field	nanoteslas

APPENDIX C ANOMALY ARCHIVE DEFINITION

Electromagnetic Anomaly Data

The electromagnetic anomaly data are provided in two formats, one ASCII and one binary:

FNNS1ANOMALY.csv – ASCII comma-delimited Excel® format (Main Block)

FNNS1ANOMALY.gdb – Geosoft® OASIS montaj binary database file (Main Block)

FNNS2ANOMALY.csv – ASCII s comma-delimited Excel® format (North Block)

FNNS2ANOMALY.gdb – Geosoft® OASIS montaj binary database file (North Block)

Both file types contain the same set of data channels, summarized as follows:

Channel Name	Description	Units
x_nad83	easting in UTM co-ordinates using NAD83 datum	metres
y_nad83	northing in UTM co-ordinates using NAD83 datum	metres
lon_nad83	longitude using NAD83 datum	decimal-degrees
lat_nad83	latitude using NAD83 datum	decimal-degrees
dem	digital elevation model	metres above sea level
fiducial	fiducial	
flight	flight number	
line_number	full flightline number	
time_utc	UTC time	seconds
time_local	local time (Central Standard Time)	seconds
date	local date	YYYYMMDD
em_x_final_on	filtered dB/dt, X-component, on-time	picoteslas per second
em_x_final_off	filtered dB/dt, X-component, off-time	picoteslas per second
em_y_final_on	filtered dB/dt, Y-component, on-time	picoteslas per second
em_y_final_off	filtered dB/dt, Y-component, off-time	picoteslas per second
em_z_final_on	filtered dB/dt, Z-component, on-time	picoteslas per second
em_z_final_off	filtered dB/dt, Z-component, off-time	picoteslas per second
em_bx_final_on	filtered B-field, X-component, on-time	femtoteslas
em_bx_final_off	filtered B-field, X-component, off-time	femtoteslas
em_by_final_on	filtered B-field, Y-component, on-time	femtoteslas
em_by_final_off	filtered B-field, Y-component, off-time	femtoteslas
em_bz_final_on	filtered B-field, Z-component, on-time	femtoteslas
em_bz_final_off	filtered B-field, Z-component, off-time	femtoteslas
tau_x	decay constant (tau) for X-component	microseconds
tau_z	decay constant (tau) for Z-component	microseconds
conductance	apparent conductance	millisiemens
height_em	electromagnetic receiver height	metres above terrain
anomaly_letter	anomaly along the survey line (A,B,C ...)	
anomaly_no	anomaly along the survey line (1,2,3 ...)	
anomaly_id	unique anomaly identifier	
survey_number	MNDM unique survey number	
anomaly_type_letter	anomaly classification	
anomaly_type_no	anomaly classification	
no_channel	number of off-time channels deflected	
conductance_vert	conductance of vertical plate model	siemens

depth	depth of vertical plate model	metres
heading	direction of flight	degrees

The unique anomaly identifier (anomaly_id) is a string in the format LLLLLA where 'LLLLL' holds the line number. The 'A' represents the anomaly letter for that line. Anomaly letters are uppercase for normal anomalies and lowercase for cultural anomalies and increase alphabetically on each line. So for example anomaly_id 10270D is the fourth normal anomaly on line 10270 and anomaly_id 12450c is the third cultural anomaly on line 12450.

The codes for anomaly_type_letter and anomaly_type_no are as follows:

N	1	Normal (bedrock) response
N?	2	Normal (bedrock) response, questionable
S	3	Surficial response
S?	4	Surficial response, questionable
C	5	Cultural (man-made) response
C?	6	Cultural (man-made) response, questionable

The (?) does not question the existence of the anomaly, but denoted some uncertainty as to the possible origin of the source.

N: Bedrock (normal) - an anomaly whose response matches that of a bedrock conductor, using a thin vertical plate model. This anomaly type might include other shapes of conductors: roughly pod-shaped, thick dykes, short strike length bodies, or conductors sub-parallel to the flight path.

S: Flat lying conductors - generally surficial. Typical geologic anomalies might be conductive overburden, swamps or clay layers. They would not appear to be conductive at depth.

C: Line current - an anomaly with the shape typical of line currents - typically cultural (man-made sources) such as power lines, train tracks, fences, etc.

The anomaly_letter proceeds in the sequence A, B, C ... Y, Z, AA, BB ... for each survey line, and correspond with the anomaly_no 1, 2, 3... 25, 26, 27, 28 Cultural anomalies are lettered separately as a, b, c ... with corresponding numbers 1, 2, 3

APPENDIX D KEATING CORRELATION ARCHIVE DEFINITION

Kimberlite Pipe Correlation Coefficients

The Keating kimberlite pipe correlation coefficient data are provided in two formats, one ASCII and one binary:

FNNSKC.csv – ASCII comma-delimited Excel® format

FNNSKC.gdb – Geosoft® OASIS montaj binary database file

Both file types contain the same set of data channels, summarized as follows:

Channel Name	Description	Units
x_nad83	easting in UTM co-ordinates using NAD83 datum	metres
y_nad83	northing in UTM co-ordinates using NAD83 datum	metres
lon_nad83	longitude using NAD83 datum	decimal-degrees
lat_nad83	latitude using NAD83 datum	decimal-degrees
corr_coeff	correlation coefficient	percent x 10
pos_coeff	positive correlation coefficient	percent
neg_coeff	negative correlation coefficient	percent
norm_error	standard error normalized to amplitude	percent
amplitude	peak-to-peak anomaly amplitude within window	nanoteslas

APPENDIX E GRID ARCHIVE DEFINITION

Gridded Data

The gridded data are provided in two formats, one ASCII and one binary:

- *.gxf - Geosoft® ASCII Grid eXchange Format (no compression)
- *.grd - Geosoft® OASIS montaj binary grid file (no compression)

The grids are summarized as follows:

- All grids are NAD83 UTM Zone 15 North, with a grid cell size of 40 m x 40 m.

Main (1) and North (2) Individual Blocks

FNNS1MAG83.grd/.gxf and FNNS2MAG83.grd/.gxf – GSC Levelled Residual Magnetic Intensity

FNNS12VD83.grd/.gxf and FNNS22VD83.grd/.gxf – Second Vertical Derivative of GSC Levelled Residual Magnetic Intensity

FNNS1DEM83.grd/.gxf and FNNS2DEM83.grd/.gxf – Digital Elevation Model

FNNS1DCX83.grd/.gxf and FNNS2DCX83.grd/.gxf – X-coil Decay Constant

FNNS1DCXDE83.grd/.gxf and FNNS2DCXDE83.grd/.gxf – X-coil Decay Constant (de-herringboned)

FNNS1DCZ83.grd/.gxf and FNNS2DCZ83.grd/.gxf – Z-coil Decay Constant

FNNS1DCZDE83.grd/.gxf and FNNS2DCZDE83.grd/.gxf – Z-coil Decay Constant (de-herringboned)

FNNS1CON83.grd/.gxf and FNNS2CON83.grd/.gxf – Apparent Conductance

FNNS1CONML83.grd/.gxf and FNNS2CONML83.grd/.gxf – Apparent Conductance (microlevelled)

FNNS1CONDE83.grd/.gxf and FNNS2CONDE83.grd/.gxf – Apparent Conductance (microlevelled and de-herringboned)

Main and North Merged for Maps

FNNS12MAG83.grd/.gxf – GSC Levelled Residual Magnetic Intensity

FNNS122VD83.grd/.gxf – Second Vertical Derivative of GSC Levelled Residual Magnetic Intensity

FNNS12DEM83.grd/.gxf – Digital Elevation Model

FNNS12DCXDE83.grd/.gxf – X-coil Decay Constant (de-herringboned)

FNNS12DCZDE83.grd/.gxf – Z-coil Decay Constant (de-herringboned)

FNNS12CONDE83.grd/.gxf – Apparent Conductance (microlevelled and de-herringboned)

APPENDIX F GEOTIFF AND VECTOR ARCHIVE DEFINITION

GeoTIFF Images

Geographically referenced colour images, incorporating a base map, are provided in GeoTIFF format for use in GIS applications:

FNNSMAG83.tif/.ipj – GSC Levelled Residual Magnetic Intensity
FNNS2VD83.tif/.ipj – Second Vertical Derivative of GSC Levelled Residual Magnetic Intensity
FNNSDCXDE83.tif/.ipj – X Coil Decay Constant (de-herringboned)
FNNSCONDDE83.tif/.ipj – Apparent Conductance (microlevelled and de-herringboned)

Vector Archives

Vector line work from the maps is provided in DXF (v12) ASCII format using the following naming convention:

FNNS1PATH83.DXF – flight path of the survey area (Main Block)
FNNS2PATH83.DXF – flight path of the survey area (North Block)
FNNS1EM83.DXF – electromagnetic anomalies (Main Block)
FNNS2EM83.DXF – electromagnetic anomalies (North Block)
FNNSKC83.DXF – Keating correlation targets (merged blocks)
FNNS12MAG83.DXF – contours of the residual magnetic intensity in nanoteslas (merged blocks)
FNNS12DCXDE83.DXF – contours of the X-coil decay constant (de-herringboned) in microseconds (merged blocks)
FNNS12CONDE83.DXF – contours of the apparent conductance (microlevelled and de-herringboned) in millisiemens (merged blocks)

The layers within the DXF files correspond to the various object types found therein and have intuitive names.

APPENDIX G TDEM PARAMETER TABLE DEFINITION

A parameter table file exists for each survey flight. This file represents the TDEM reference waveform used by the system to compensate the received signal for the contribution by the primary field generated at the transmitter.

Each file is stored as "PTAxxx.out", where xxx identifies the corresponding flight number.

The files are archived as standard ASCII text files and contain the following information:

- System geometry/configuration.
- Window (channel) positions, given in samples along the waveform.
- Conversion factors from listed values to PPM.
- Each point of the waveform for the following 7 components:
 - Transmitter response in units of Am²
 - dB/dt X-coil response in units of nT/s
 - dB/dt Y-coil response in units of nT/s
 - dB/dt Z-coil response in units of nT/s
 - B-Field X-coil response in units of pT
 - B-Field Y-coil response in units of pT
 - B-Field Z-coil response in units of pT

A sample of a parameter table follows:

GEOTEM Calibration Data - Version 31 July 1998

'D0080112.002' = Name of original saved parameter table file

125.000000000000000 = Horizontal TX-RX separation in metres

50.000000000000000 = Vertical TX-RX separation in metres

90.000000000000000 = Base Frequency in Hertz

43.40277777777780 = Sample Interval in micro-seconds

20 Time Gates: First and Last Sample number, RMS chart position:

1	4	10	1
2	11	23	2
3	24	36	3
4	37	49	4
5	50	53	5
6	54	55	6
7	56	58	7
8	58	61	8
9	62	64	9
10	65	68	10
11	69	72	11
12	73	76	12
13	77	81	13
14	82	86	14
15	87	91	15
16	92	97	16
17	98	103	17
18	104	110	18
19	111	118	19
20	119	128	20

Component:	TX	dBx/dt	dBy/dt	dBz/dt	Bx	By	Bz
IndivPPM:		16.97154	852.8368	32.88570	24.99176	1302.157	48.35992
TotalPPM:		15.07923	15.07923	15.07923	22.19901	22.19901	22.19901
SI_Units:		1.000000	1.000000	1.000000	1.000000	1.000000	1.000000
DataUnits: A*m^2		nT/s	nT/s	nT/s	pT	pT	pT
128 Samples:							
1	7729.282	15.96003	-3.930862	25.94668	-113.2370	-.2736754	-53.69548
2	1024.003	24.50268	1.026651	13.67564	-112.3589	-.3367008	-52.83562
3	398.5879	317.5182	16.88734	198.6653	-104.9366	.5205769E-01	-48.22753
4	15695.36	3616.584	119.4898	2086.784	-19.56110	3.011632	1.369888
5	67698.08	14473.86	379.0306	7872.654	373.0266	13.83022	217.5035
6	134235.2	30133.23	732.3142	15838.12	1341.062	37.94794	732.0602
7	198690.4	43453.41	1017.253	22496.55	2937.995	75.91598	1563.976
8	261714.8	51975.27	1164.056	26779.31	5008.929	123.2534	2633.330
9	323187.0	56594.40	1207.164	29131.60	7365.042	174.7122	3846.675
10	382890.4	58589.26	1196.222	30170.94	9864.688	226.8690	5133.622
11	440686.7	58926.92	1161.745	30367.83	12414.95	278.0401	6447.398
12	496231.2	58214.87	1118.357	30021.63	14957.09	327.5215	7757.933
13	549314.6	56810.41	1071.185	29312.33	17453.30	375.0376	9045.562
14	599686.2	54918.71	1021.773	28345.43	19877.98	420.4577	10296.82
15	647069.8	52657.67	969.9995	27182.63	22212.53	463.6819	11501.85
16	691302.4	50094.17	915.6895	25860.95	24442.39	504.6040	12652.97
17	732240.1	47272.43	857.8681	24404.12	26555.38	543.0926	13743.79
18	769640.8	44222.05	796.7552	22827.58	28540.94	579.0003	14768.79
19	803450.5	40966.94	731.9139	21144.64	30389.66	612.1745	15723.04
20	833346.6	37527.52	663.6411	19366.39	32093.10	642.4600	16602.19
21	859323.9	33922.85	592.5283	17502.52	33643.67	669.7206	17402.30
22	881209.9	30170.38	518.8977	15562.19	35034.58	693.8401	18119.85
23	898976.3	26288.71	442.1611	13555.16	36259.82	714.6964	18751.73
24	912502.6	22297.01	364.2277	11491.54	37314.20	732.1962	19295.28
25	921742.5	18214.65	284.6580	9381.562	38193.36	746.2779	19748.26
26	926662.2	14060.86	204.0446	7234.495	38893.78	756.8834	20108.85
27	927364.1	9854.848	122.9833	5060.035	39412.79	763.9804	20375.66
28	923746.7	5615.631	41.92896	2869.674	39748.52	767.5592	20547.74
29	915895.0	1362.764	-39.14478	671.1644	39899.96	767.6196	20624.58
30	903873.7	-2884.436	-121.0489	-1523.952	39866.93	764.1432	20606.08
31	887685.5	-7103.616	-201.4232	-3703.113	39650.18	757.1451	20492.64
32	867399.8	-11277.36	-280.4637	-5859.924	39251.29	746.6875	20285.11
33	843172.9	-15386.93	-357.6422	-7983.167	38672.64	732.8397	19984.70
34	815163.6	-19412.59	-433.1687	-10062.68	37917.44	715.6780	19593.08
35	783413.8	-23336.08	-506.9882	-12089.16	36989.73	695.2753	19112.35
36	748179.8	-27139.86	-578.1486	-14054.79	35894.33	671.7263	18544.99
37	709579.2	-30807.27	-647.4260	-15948.87	34636.80	645.1296	17893.87
38	667809.9	-34320.21	-712.1000	-17762.84	33223.44	615.6260	17162.28
39	623115.9	-37664.14	-773.0846	-19489.75	31661.28	583.3955	16353.85
40	575678.5	-40823.00	-830.5354	-21120.95	29958.00	548.5947	15472.54
41	525725.8	-43783.54	-884.4982	-22649.47	28121.92	511.3761	14522.66
42	473492.1	-46532.31	-933.8410	-24068.54	26161.94	471.9156	13508.81
43	419244.9	-49057.47	-978.6750	-25371.42	24087.51	430.4113	12435.90
44	363220.0	-51347.62	-1018.960	-26553.29	21908.58	387.0599	11309.06
45	305690.8	-53393.00	-1054.490	-27608.78	19635.57	342.0632	10133.67
46	247003.6	-55184.48	-1085.077	-28533.00	17279.28	295.6316	8915.313
47	187352.1	-56715.41	-1110.876	-29322.47	14850.90	247.9763	7659.769
48	127010.4	-57979.32	-1131.085	-29974.13	12361.87	199.3227	6372.951
49	65108.98	-58917.41	-1137.950	-30448.89	9825.045	150.0814	5061.687
50	8325.732	-58320.01	-1086.630	-30032.90	7280.830	101.8049	3749.149
51	-14672.06	-51573.19	-916.9132	-26305.74	4895.995	58.32526	2526.522

52	-10537.82	-37103.35	-593.0906	-18811.49	2971.591	25.55608	1547.415
53	-5599.680	-21897.11	-243.9040	-11197.24	1691.199	7.392134	896.1842
54	-3335.518	-11422.98	-34.09738	-5971.165	968.1067	1.359118	523.6060
55	-2195.035	-5555.815	40.83756	-2999.166	599.6433	1.505389	328.9374
56	-1650.604	-2597.416	46.96001	-1462.370	422.7069	3.410719	232.1159
57	-1394.167	-1207.738	31.18607	-714.3275	340.1297	5.106597	184.8785
58	-1290.904	-587.9979	14.44187	-364.0430	301.1598	6.096787	161.4764
59	-1259.885	-325.6664	2.467782	-205.2027	281.3320	6.463750	149.1229
60	-1249.743	-219.5141	-4.727469	-135.2952	269.5008	6.414712	141.7337
61	-1236.130	-178.4729	-7.894109	-105.1228	260.8640	6.140806	136.5163
62	-1228.445	-162.4722	-8.681833	-91.96437	253.4650	5.781085	132.2392
63	-1228.072	-154.7766	-8.449795	-85.45306	246.5802	5.409305	128.3890
64	-1235.436	-149.0760	-7.719331	-81.20456	239.9862	5.058412	124.7723
65	-1239.135	-143.7213	-6.716692	-77.92262	233.6321	4.745131	121.3190
66	-1228.420	-138.4068	-5.746719	-75.17229	227.5095	4.474657	117.9966
67	-1230.271	-132.8315	-5.199392	-72.73333	221.6233	4.237111	114.7869
68	-1230.279	-127.4344	-4.822192	-69.75897	215.9752	4.019629	111.6946
69	-1232.587	-121.9220	-4.375208	-66.75803	210.5638	3.820033	108.7320
70	-1231.816	-116.5951	-3.843931	-64.03566	205.3876	3.641666	105.8936
71	-1230.655	-111.5820	-3.492133	-61.65565	200.4359	3.482463	103.1659
72	-1240.686	-106.7221	-3.285778	-59.28498	195.6984	3.335373	100.5413
73	-1230.556	-102.1274	-2.788408	-56.58284	191.1660	3.203555	98.02684
74	-1224.671	-97.80101	-2.555312	-54.35416	186.8273	3.087589	95.61935
75	-1242.676	-93.79646	-2.602747	-52.20010	182.6694	2.975652	93.30698
76	-1221.913	-90.06383	-2.423037	-49.80333	178.6794	2.866585	91.09336
77	-1224.827	-86.67500	-2.085020	-47.63036	174.8439	2.768754	88.97892
78	-1223.877	-83.54163	-2.145144	-45.92556	171.1499	2.676954	86.94862
79	-1224.360	-80.37018	-2.181369	-43.74102	167.5928	2.583062	85.00273
80	-1216.329	-77.45803	-2.054077	-42.29580	164.1677	2.491147	83.13562
81	-1216.461	-74.63999	-1.909674	-41.02884	160.8670	2.405128	81.32736
82	-1219.590	-71.84667	-1.952082	-39.22677	157.6880	2.321323	79.58570
83	-1217.326	-69.29994	-1.722317	-37.73324	154.6250	2.241583	77.91556
84	-1208.074	-66.98568	-1.702209	-36.93633	151.6674	2.167266	76.29512
85	-1204.960	-64.85393	-1.863035	-35.93988	148.8063	2.089895	74.71361
86	-1212.486	-62.79464	-1.811555	-34.36544	146.0361	2.010152	73.18789
87	-1197.069	-61.05624	-1.531892	-33.37806	143.3484	1.937594	71.71776
88	-1200.950	-59.26998	-1.342465	-32.39280	140.7371	1.875217	70.29044
89	-1207.054	-57.18716	-1.143159	-31.13019	138.2098	1.821275	68.91190
90	-1204.022	-55.12002	-1.410749	-29.84234	135.7726	1.765852	67.58871
91	-1208.568	-53.75584	-1.293131	-28.49288	133.4099	1.707174	66.32276
92	-1199.583	-52.40686	-1.289343	-27.83346	131.1060	1.651131	65.10040
93	-1202.806	-50.86095	-1.529696	-27.22848	128.8649	1.589954	63.90548
94	-1199.792	-49.30663	-1.576225	-26.20628	126.6912	1.522551	62.74587
95	-1199.316	-47.86020	-1.543451	-25.17110	124.5825	1.454850	61.63091
96	-1192.981	-46.37361	-1.681621	-24.67046	122.5375	1.384861	60.54928
97	-1202.529	-45.03350	-1.735938	-24.19844	120.5538	1.310695	59.48876
98	-1201.134	-43.87226	-1.298038	-23.61783	118.6245	1.244854	58.45108
99	-1196.000	-42.72894	-0.9459133	-23.08331	116.7451	1.196157	57.43760
100	-1193.117	-41.36467	-1.104402	-22.57521	114.9201	1.151662	56.44674
101	-1188.970	-40.08990	-1.055567	-21.90611	113.1525	1.104788	55.48144
102	-1191.844	-39.20676	-0.9711572	-21.28362	111.4316	1.060805	54.54416
103	-1187.353	-38.35579	-0.9610370	-20.83961	109.7484	1.018874	53.63003
104	-1182.623	-37.58065	-1.107444	-19.57735	108.1005	.9739849	52.75292
105	-1185.573	-36.67272	-1.140099	-18.58970	106.4891	.9252101	51.92465
106	-1192.319	-35.65127	-0.9681687	-18.88900	104.9195	.8794578	51.11131
107	-1181.724	-34.75552	-0.9804116	-18.50845	103.3916	.8371709	50.29973
108	-1186.438	-34.17176	-1.026308	-17.45993	101.8958	.7936223	49.51917

109	-1199.872	-33.28027	-.9290356	-17.02904	100.4320	.7511886	48.77071
110	-1188.594	-32.43866	-.9026078	-16.96322	99.00581	.7114394	48.03303
111	-1179.076	-31.71388	-1.017675	-16.18233	97.61361	.6697666	47.31372
112	-1182.215	-30.66168	-.9334908	-15.89610	96.25997	.6274236	46.61758
113	-1180.092	-29.68911	-.8826723	-16.25654	94.95028	.5880103	45.91982
114	-1187.398	-29.09322	-.9129155	-15.74467	93.67462	.5490436	45.22535
115	-1177.059	-28.75610	-1.009828	-14.67370	92.41921	.5073174	44.56523
116	-1174.586	-28.25669	-.9648259	-14.49814	91.18195	.4644646	43.93216
117	-1183.997	-27.73846	-.9766050	-14.75480	89.96678	.4223329	43.29733
118	-1167.828	-27.23595	-1.118851	-14.37880	88.77376	.3768586	42.66509
119	-1173.520	-26.52897	-1.165315	-13.72234	87.60698	.3272890	42.05526
120	-1169.221	-25.98087	-.8165336	-13.67054	86.46745	.2842801	41.46079
121	-1175.950	-25.32296	-.5975554	-13.33578	85.35408	.2535924	40.87472
122	-1171.817	-24.59286	-.8683287	-12.00767	84.27084	.2217807	40.32473
123	-1179.774	-24.14219	-.8897683	-11.37691	83.21322	.1836276	39.81725
124	-1171.686	-23.78949	-.2847956	-11.95205	82.17304	.1581379	39.31098
125	-1164.672	-23.16276	-.2341293	-11.92169	81.15411	.1468765	38.79289
126	-1174.168	-22.62722	-.9565273	-11.68826	80.16040	.1210376	38.28052
127	-1169.698	-22.20212	-.9646375	-11.90825	79.18754	.7934567E-01	37.76844
128	-1175.490	-21.84364	-.6305303	-11.79718	77.75765	.3104493E-01	36.99799

APPENDIX H HALFWAVE ARCHIVE DEFINITION

Each ASCII file is a continuous data stream representing the acquisition for one complete flight. Each line of the ASCII file contains 1549 data values, namely the fiducial $[F]$, and for each of the four components [T, X, Y, and Z], the primary electromagnetic field $[PEM]$, the powerline monitor $[PLM]$, the earth's field monitor (ambient electromagnetic noise) $[EFM]$ and the 384 waveform points stored in that order. The four waveform components are:

T - PEM_T, PLM_T, EFM_T and the amplitude of the transmitted electromagnetic field $[T_1...T_{384}]$

X - PEM_X, PLM_X, EFM_X and the amplitude of the secondary electromagnetic field as seen by the X-coil $[X_1...X_{384}]$

Y - PEM_Y, PLM_Y, EFM_Y and the amplitude of the secondary electromagnetic field as seen by the Y-coil $[Y_1...Y_{384}]$

Z - PEM_Z, PLM_Z, EFM_Z and the amplitude of the secondary electromagnetic field as seen by the Z-coil $[Z_1...Z_{384}]$

All data values are stored in scientific format (exponential notation), as volts. The format allows storage of the waveform as 384 points. Depending on the base frequency, if the waveform is not defined by the full 384 points, then the remaining points are simply filled with zeroes. At 90 Hz base frequency, the waveform is defined by 128 points. The halfwave sampling rate of 4 Hz is a forty five-fold stack from the original sampling rate of 90 Hz.

The fiducials mark the number of seconds after midnight for the day of the flight. Each fiducial represents a 0.25 second sample. As such, although the fiducials repeat for four lines of data, they actually increment by 0.25 seconds. For example, the second occurrence of fiducial 74087 is actually 74087.25 seconds, the third is 74087.50 seconds and the fourth is 74087.75 seconds.

The following table illustrates the ASCII data structure:

column												
1	2	3	4	5		388	389	390	391	392		775
F	PEM_T	PLM_T	EFM_T	T_1	...	T_{384}	PEM_X	PLM_X	EFM_X	X_1	...	X_{384}
volts												
74087	1.0012530E+00	9.7377970E-04	6.5032010E-04				9.9598440E-01	1.7564380E-03	-3.3043160E-03			
74087	1.0012400E+00	8.6172720E-05	7.1580250E-04				9.9651290E-01	1.7200990E-03	-6.0959600E-02			
74087	1.0012840E+00	8.7328300E-05	7.0525570E-04				9.9891420E-01	1.6912790E-03	-8.5706660E-02			
74087	1.0011300E+00	9.2401830E-05	7.4590280E-04				1.0005320E+00	2.5104030E-03	-4.9193540E-02			
column												
776	777	778	779			1162	1163	1164	1165	1166		1549
PEM_Y	PLM_Y	EFM_Y	Y_1	...	Y_{384}	PEM_Z	PLM_Z	EFM_Z	Z_1	...	Z_{384}	
volts												
-1.4667880E+00	1.9064400E-03	1.9168430E-01				1.0075570E+00	1.3699210E-03	-6.2297300E-03				
-1.4890710E+00	4.5591580E-03	-2.0755340E-03				1.0058710E+00	1.4081860E-03	7.7472150E-03				
-1.3149210E+00	1.9930260E-03	-1.6909430E-01				1.0018460E+00	1.5687660E-03	9.7720830E-03				
-1.0673150E+00	1.8790290E-03	-1.8799610E-01				9.9887660E-01	1.7389310E-03	-5.1124900E-03				

APPENDIX I MULTICOMPONENT MODELING

The results of multicomponent fixed-wing airborne EM modeling are provided for different conductor geometries as a reference for the user.

Plate Modeling

The PLATE program has been used to generate synthetic responses over a number of plate models with varying depth of burial (0, 150 and 300 m) and dips (0, 45, 90 and 135 degrees). The geometry assumed for the fixed-wing airborne EM system is shown on the following page (Figure 1), and the transmitter waveform on the subsequent page (Figure 2). In these models, the receiver is 130 m behind and 50 m below the transmitter center.

In all cases the plate has a strike length of 600m, with a strike direction into the page. The width of the plate is 300m. As the flight path traverses the center of the plate, the Y component is zero and has not been plotted.

The conductance of the plate is 20 S. In cases when the conductance is different, an indication of how the amplitudes may vary can be obtained from the nomogram included (Figure 3).

In the following profile plots (Figures 4 to 15) the plotting point is the receiver location and all of the component values are in nT/s, assuming a transmitter dipole moment of 900 000 Am². If the dipole moment is larger or smaller than 900 000 Am², then the response would be scaled up or down appropriately.

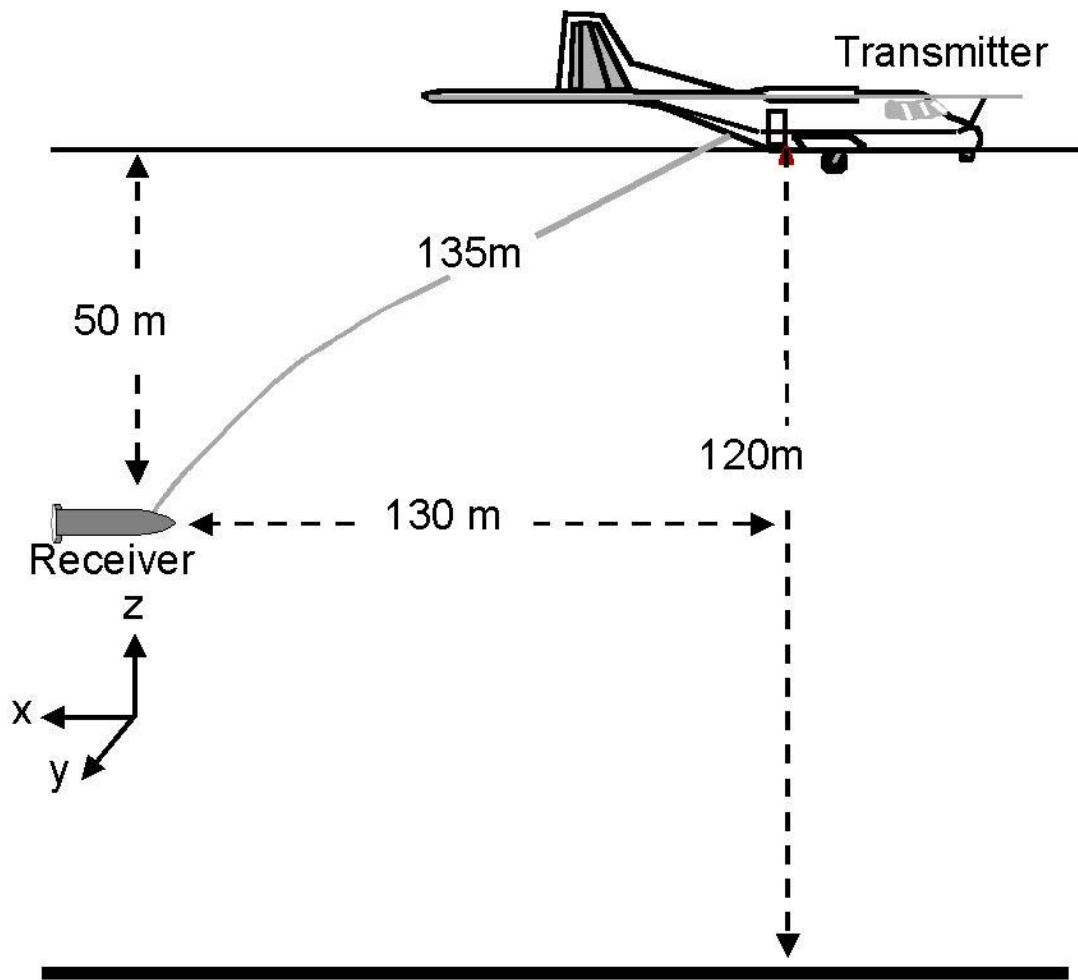


Figure 1: Nominal geometry of the MEGATEM/GEOTEM system.

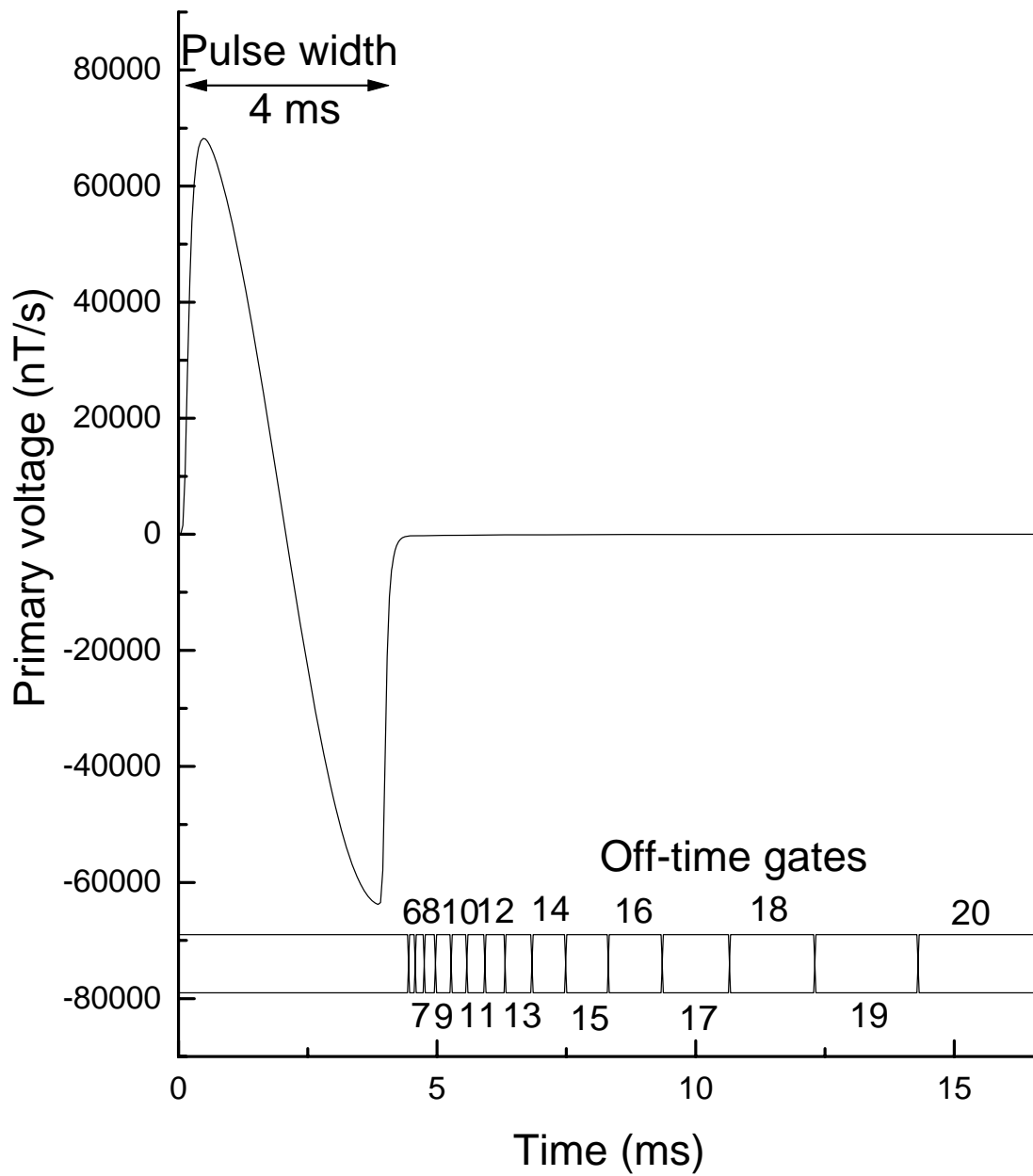


Figure 2: Theoretical transmitter waveform response in the receiver.

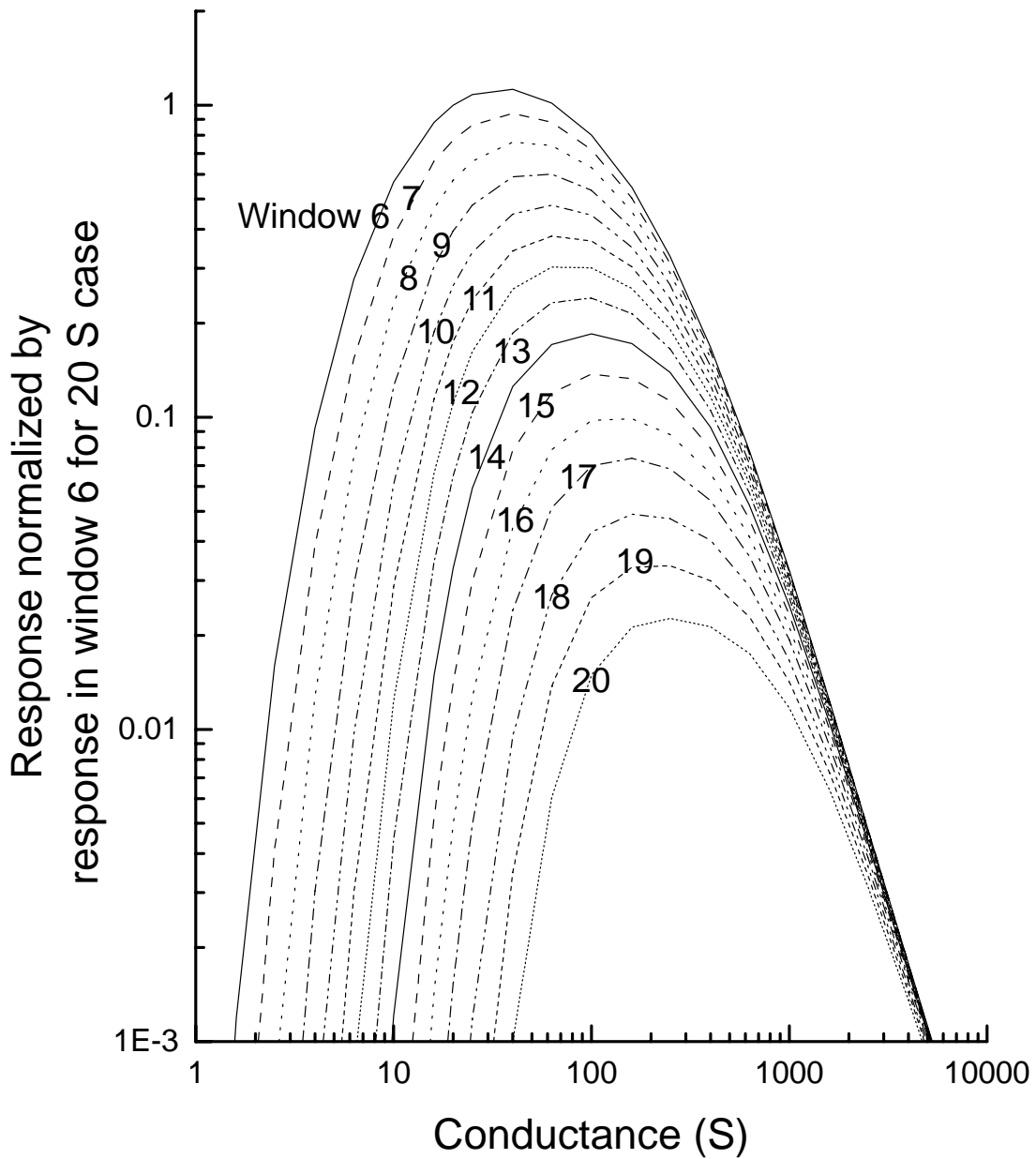


Figure 3: Nomogram for windows 6-20 normalized to a response from a 20 siemen conductor in window 6.

Plate: dip=0; depth=0

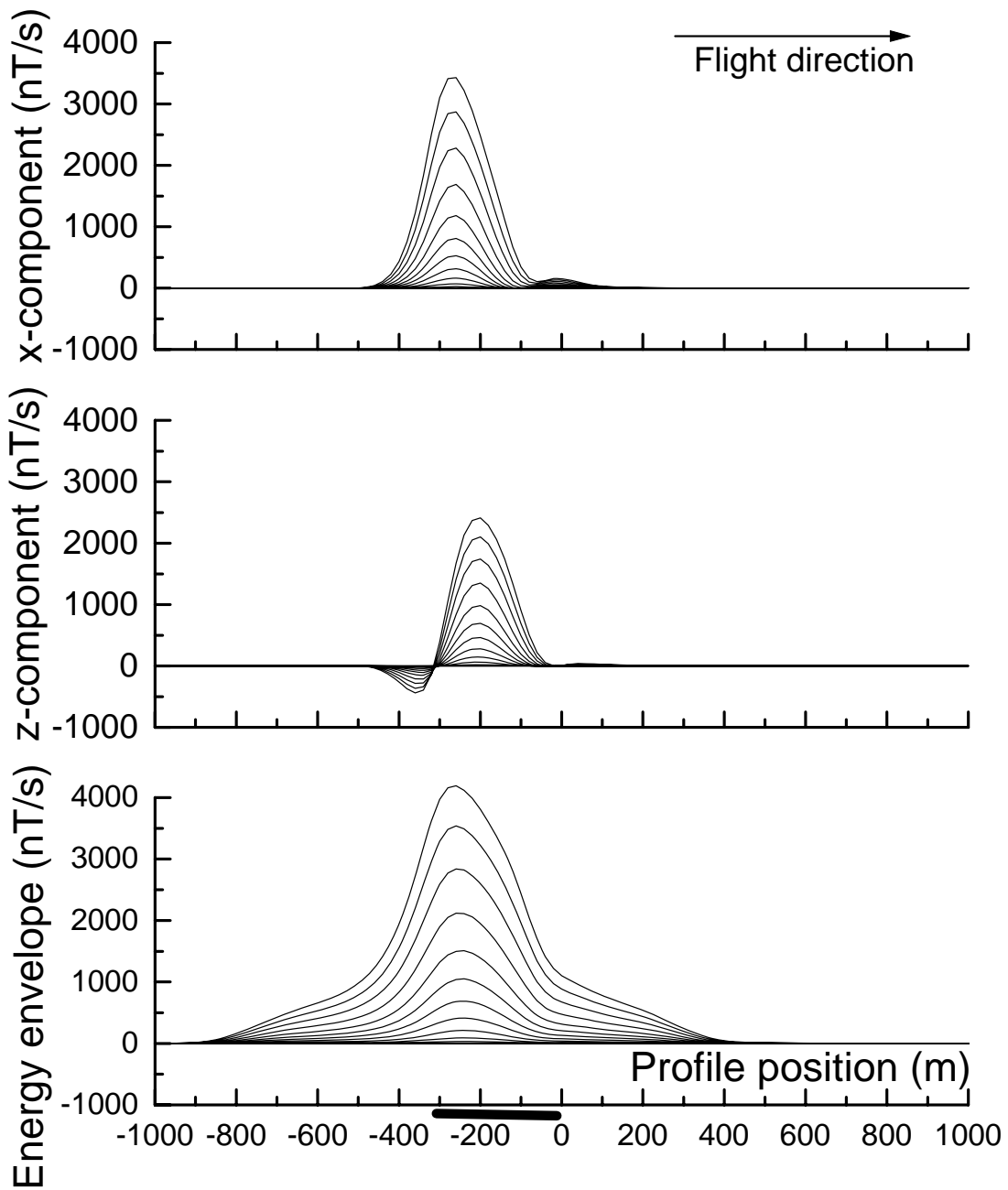


Figure 4: Flat-lying plate, depth of 0 m.

Plate: dip=0; depth=150

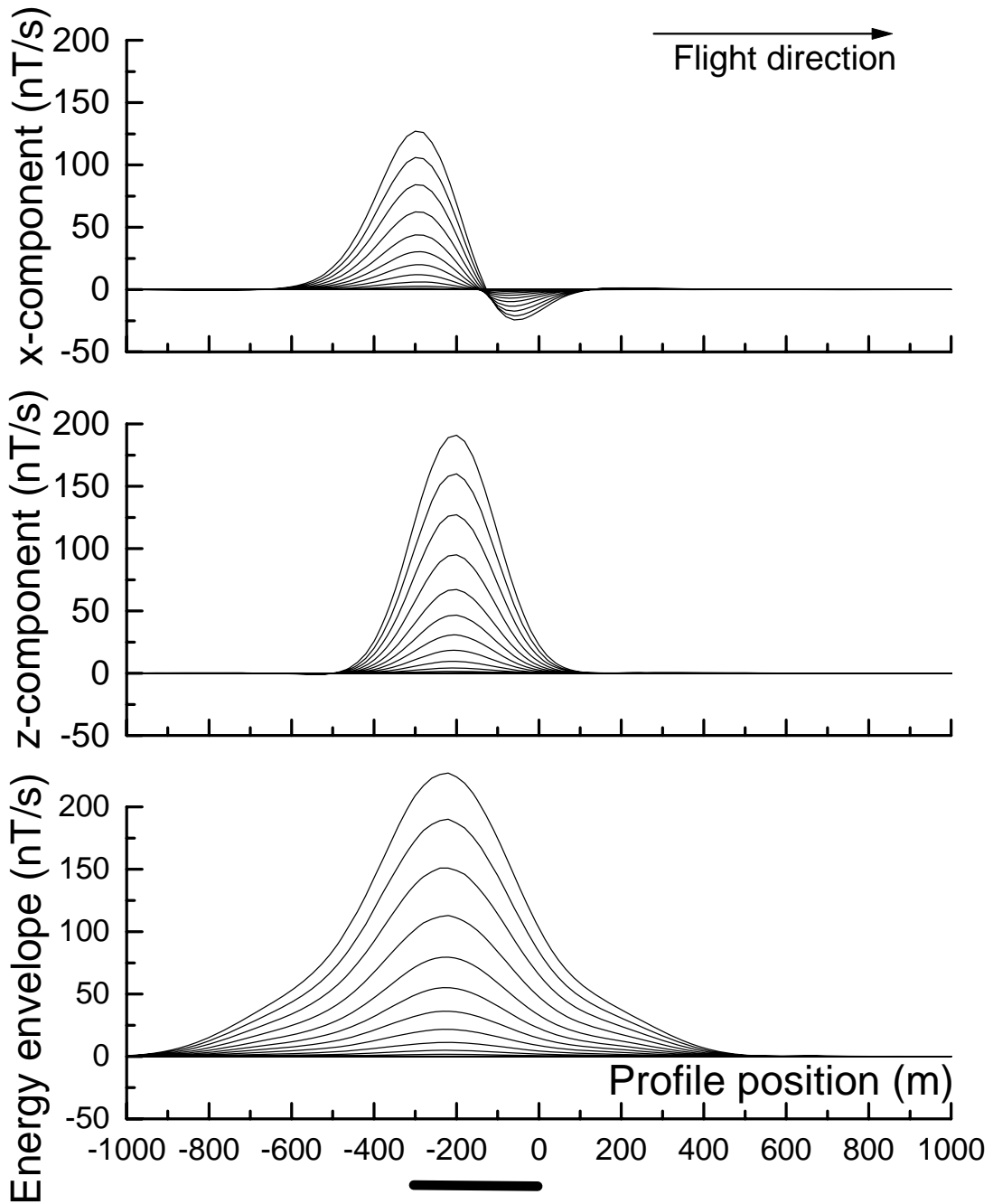


Figure 5: Flat-lying plate, depth of 150 m.

Plate: dip=0; depth=300

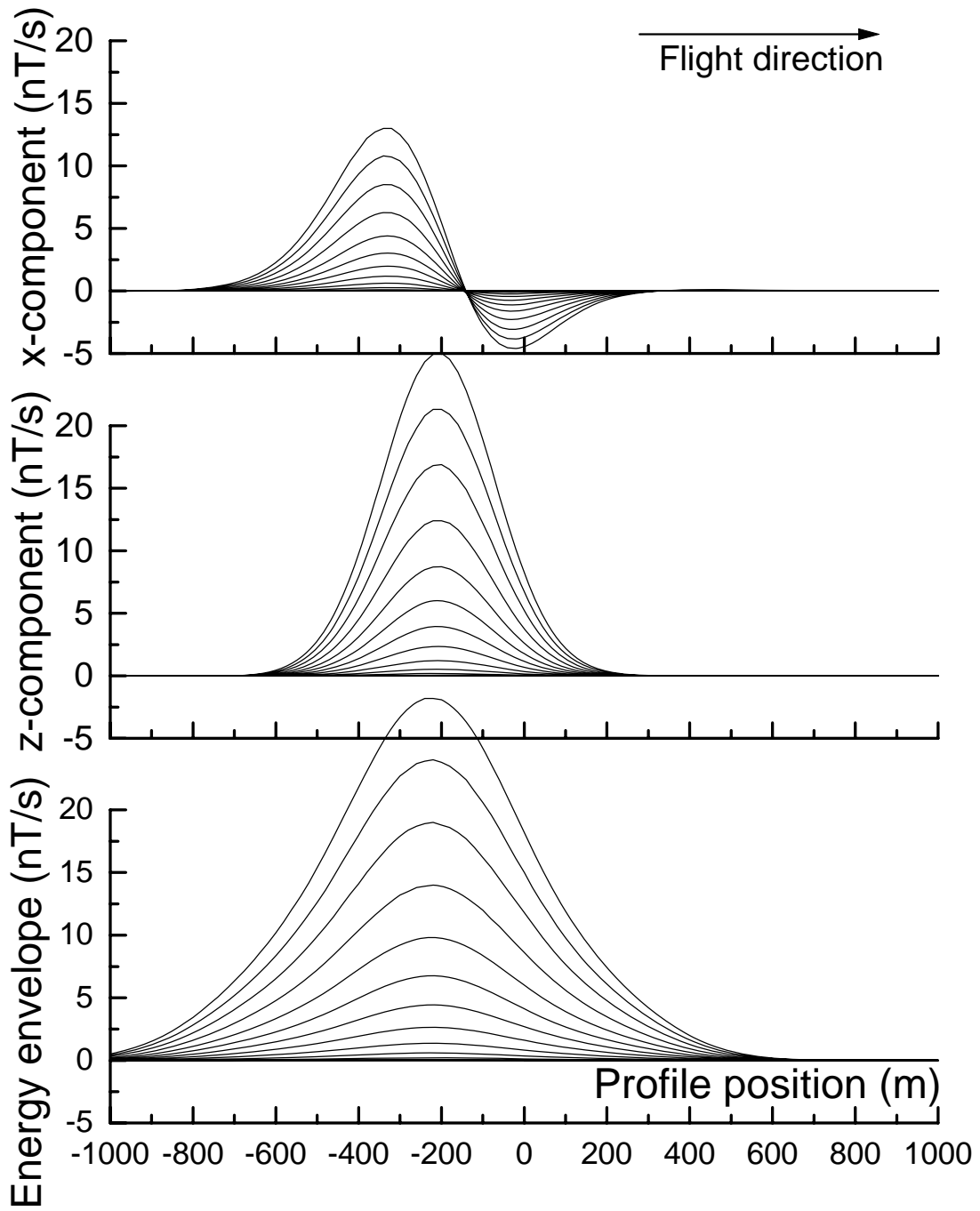


Figure 6: Flat-lying plate, depth of 300 m.

Plate: dip=45; depth=0

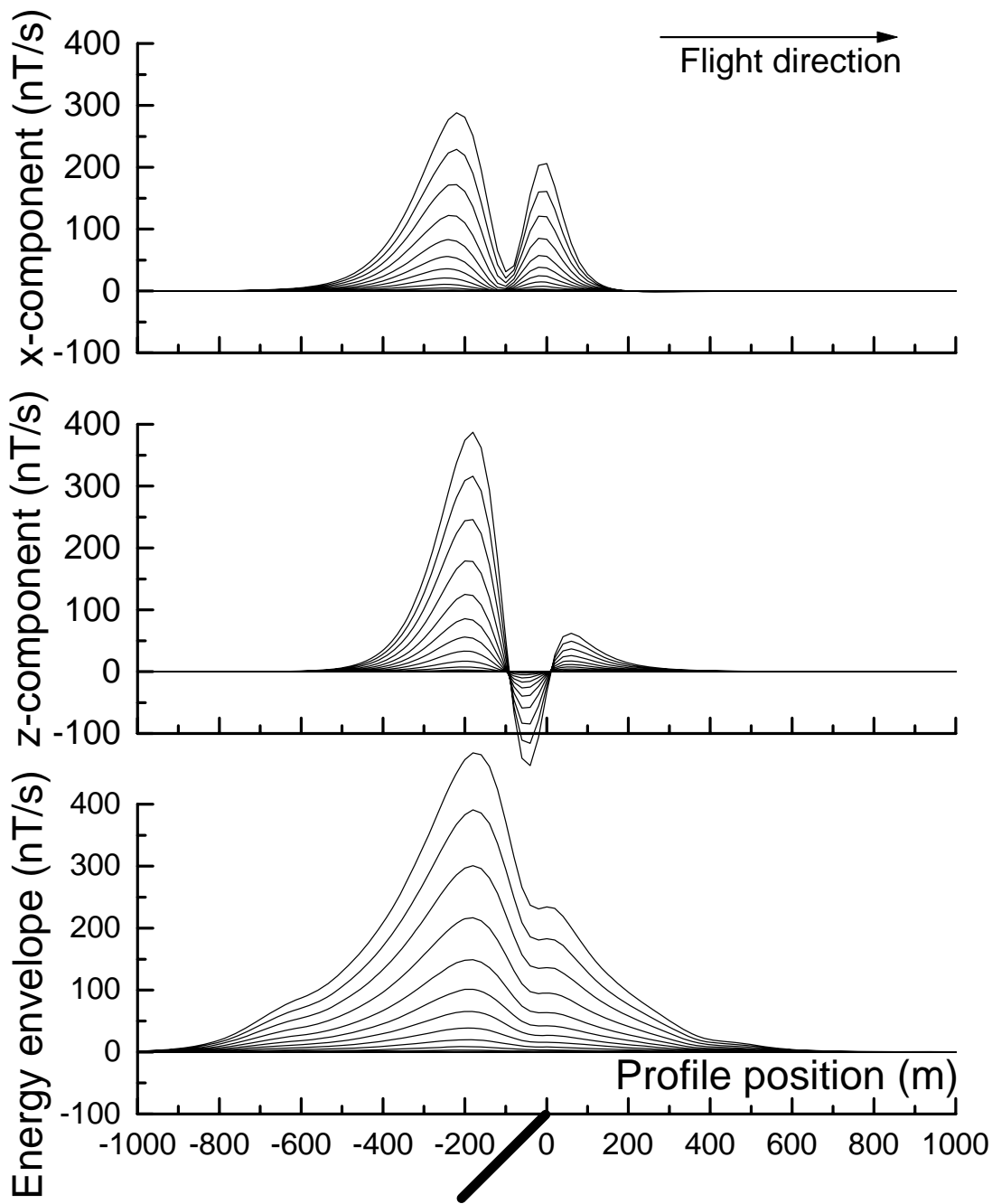


Figure 7: West-dipping plate, depth of 0 m.

Plate: dip=45; depth=150

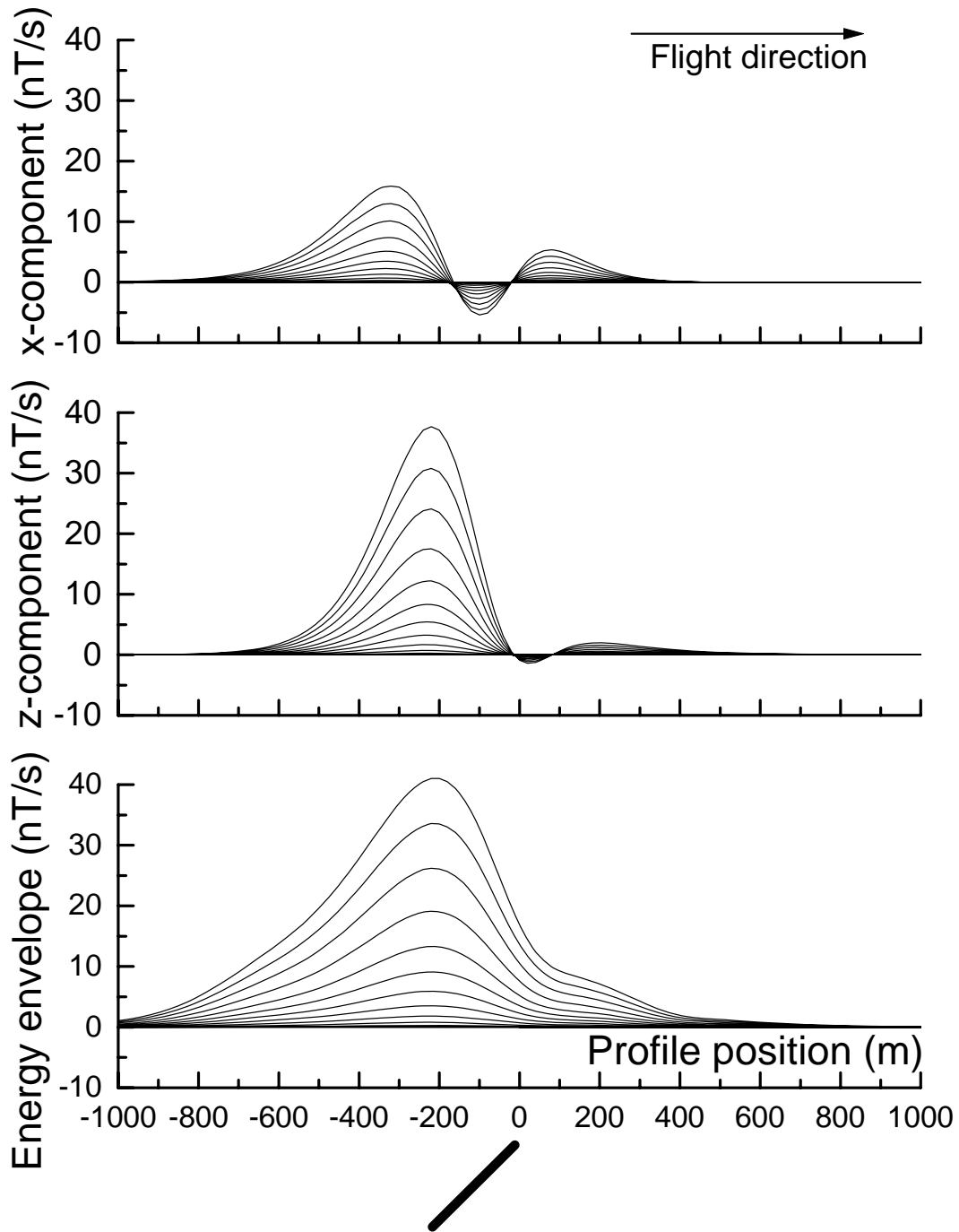


Figure 8: West-dipping plate, depth of 150 m.

Plate: dip=45; depth=300

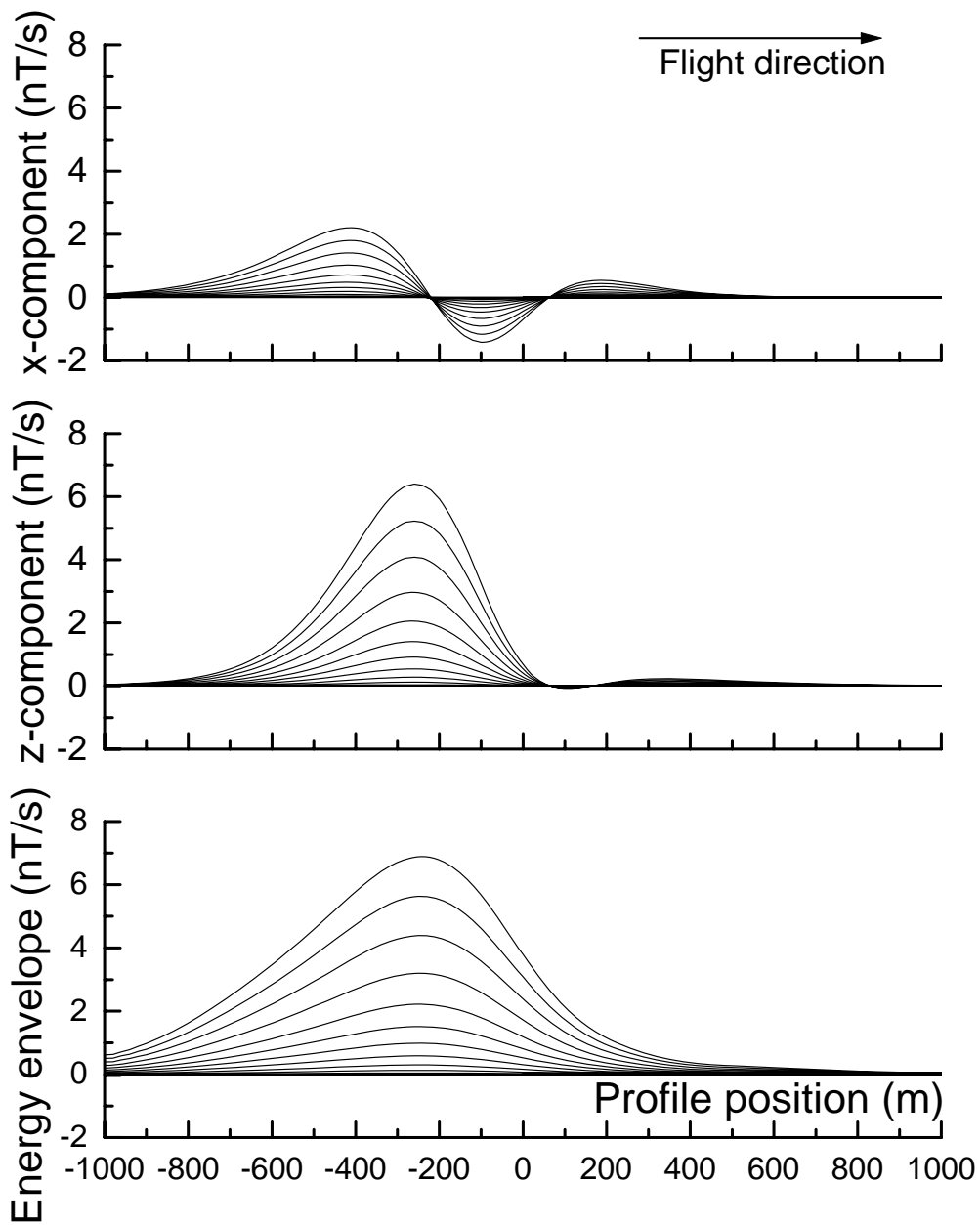


Figure 9: West-dipping plate, depth of 300 m.

Plate: dip=90; depth=0

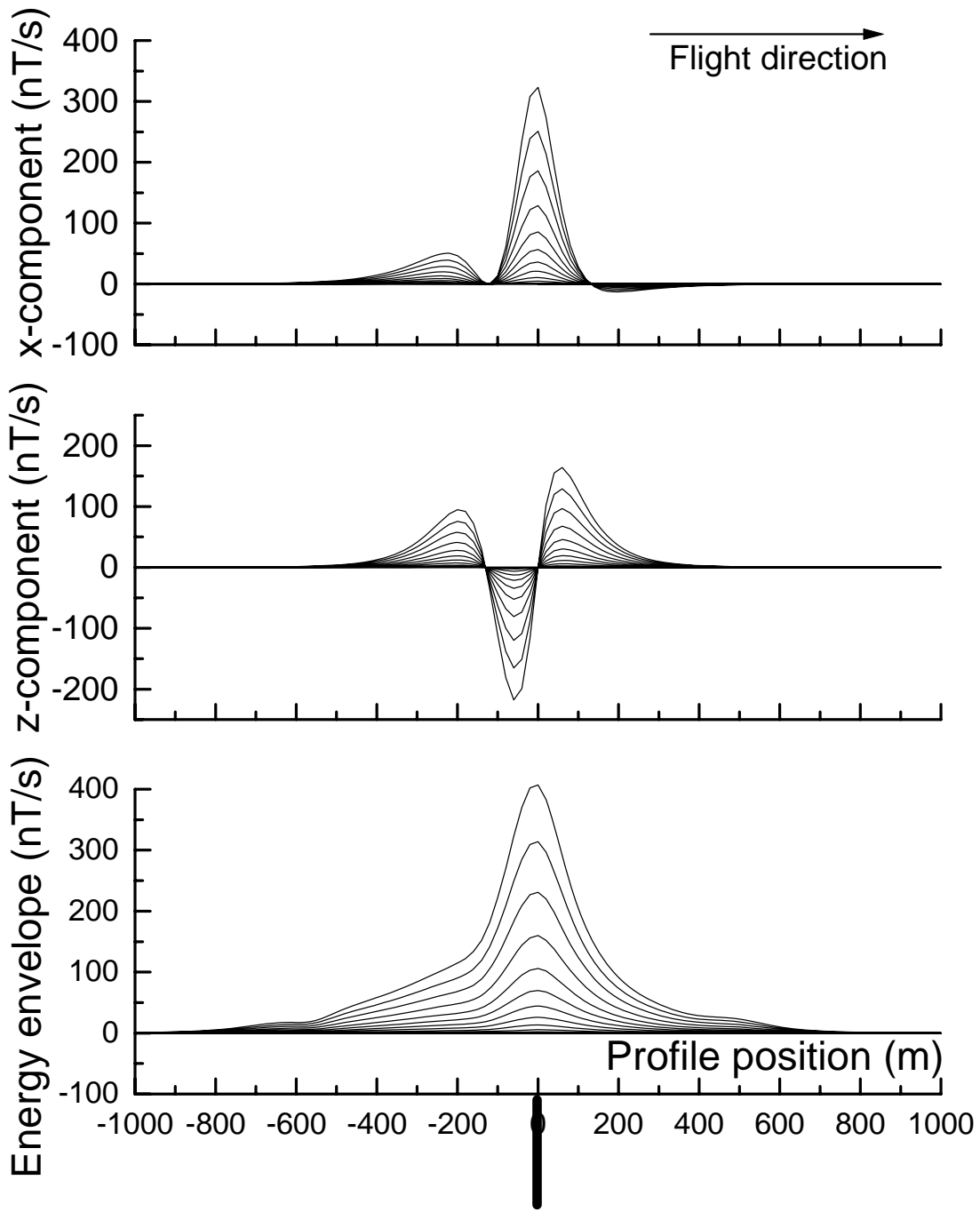


Figure 10: Vertical plate, depth of 0 m.

Plate: dip=90; depth=150

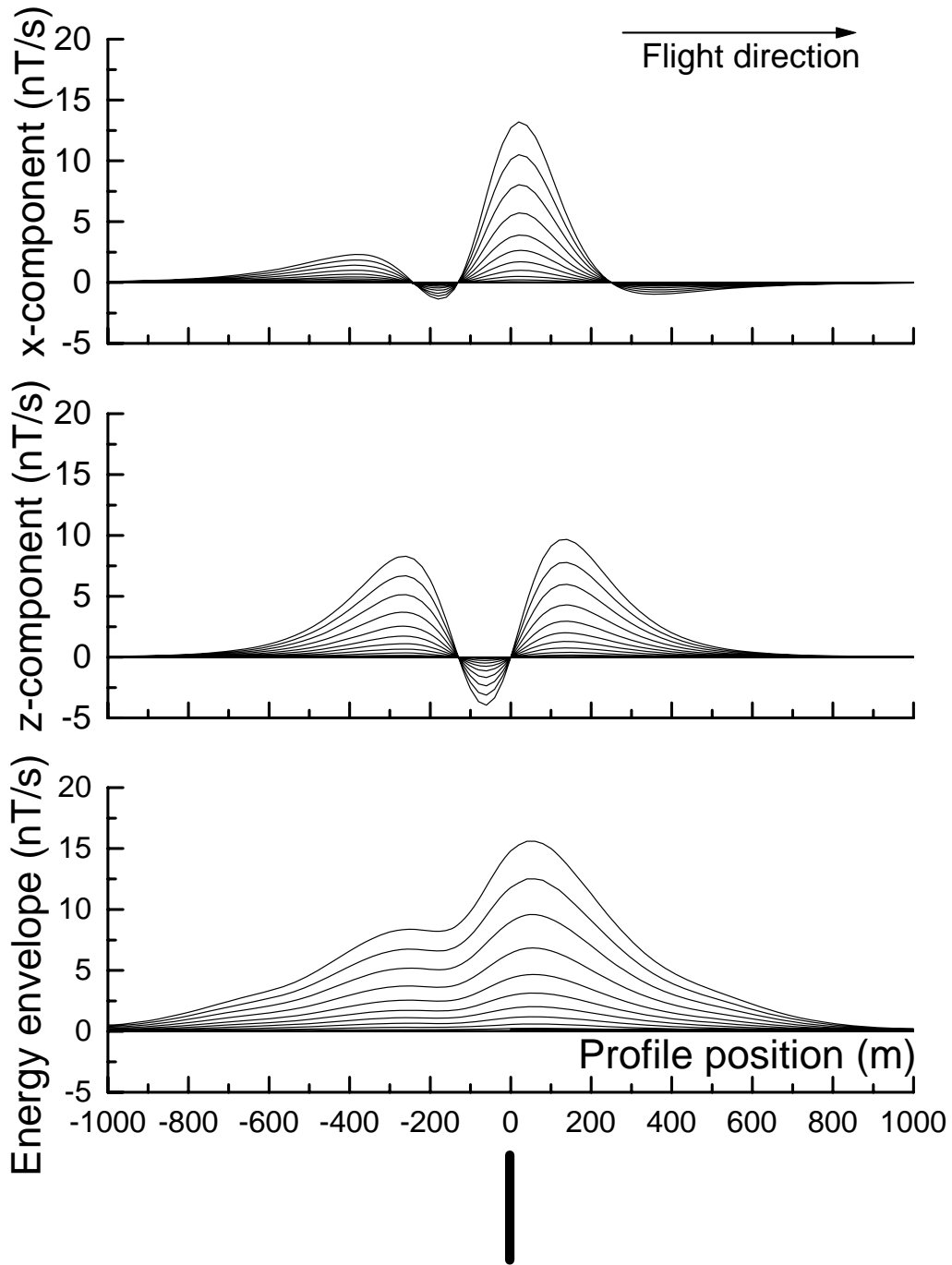


Figure 11: Vertical plate, depth of 150 m.

Plate: dip=90; depth=300

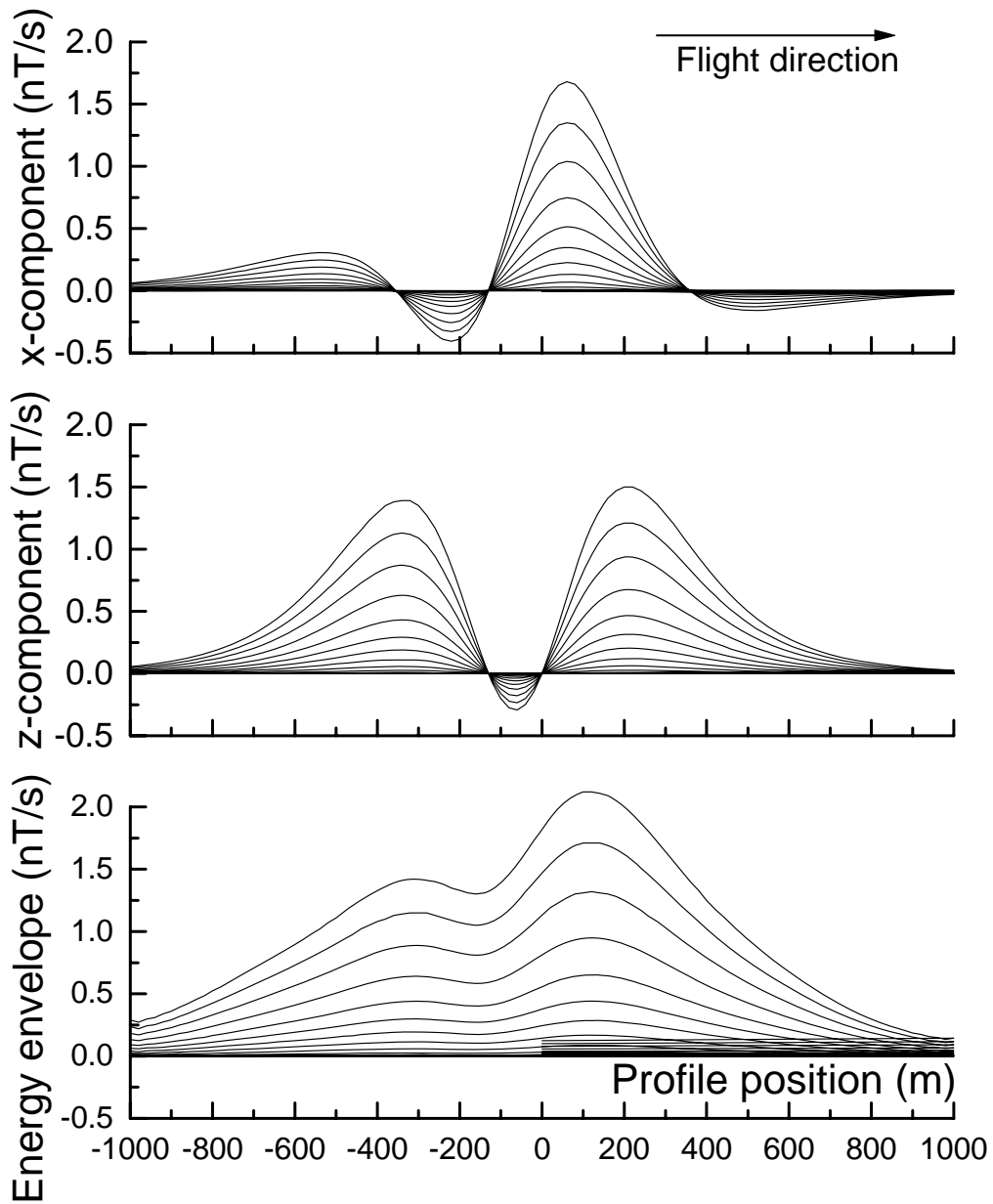


Figure 12: Vertical plate, depth of 300 m.

Plate: dip=135; depth=0

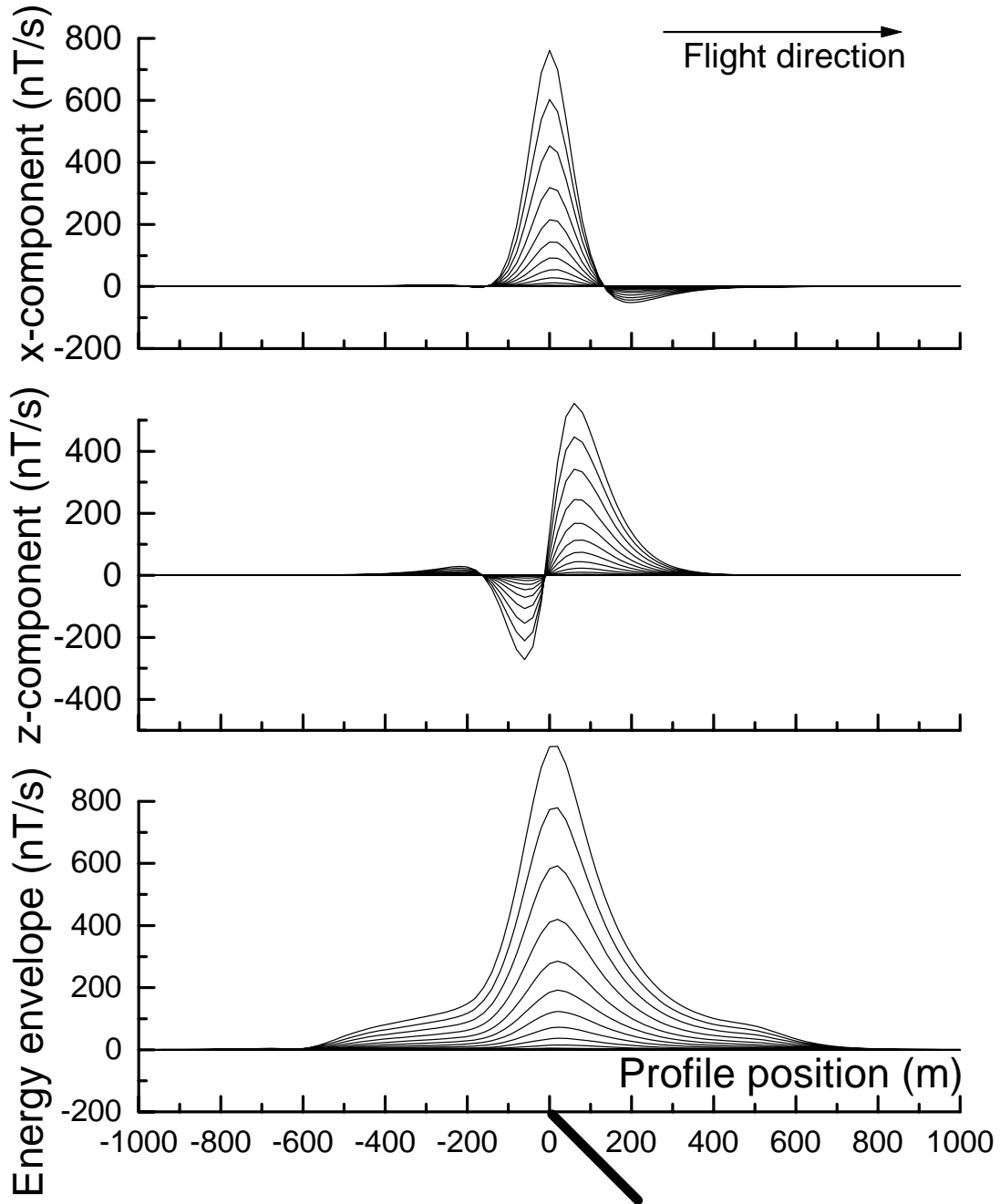


Figure 13: East-dipping plate, depth of 0 m.

Plate: dip=135; depth=150

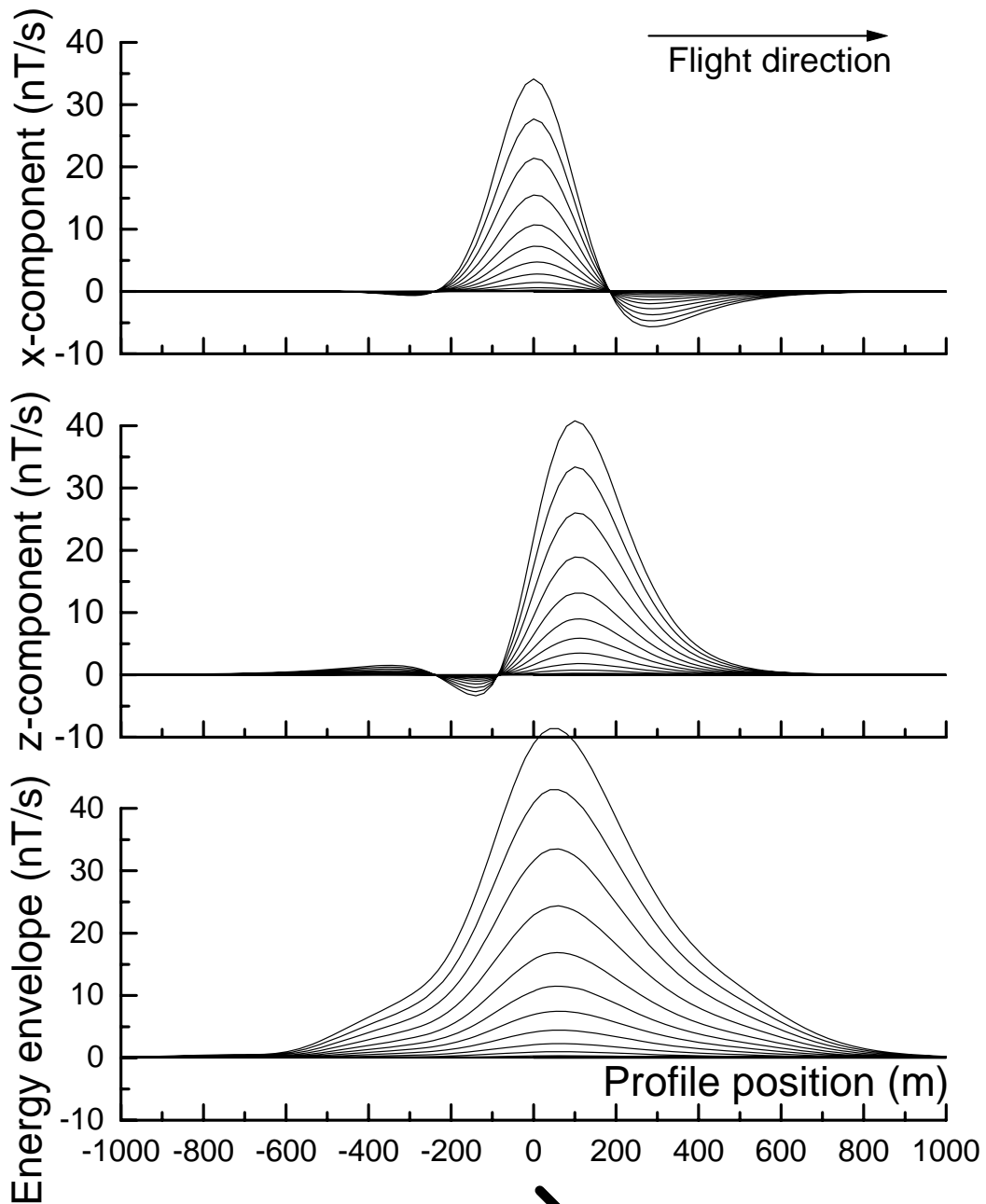


Figure 14: East-dipping plate, depth of 150 m.

Plate: dip=135; depth=300

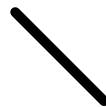
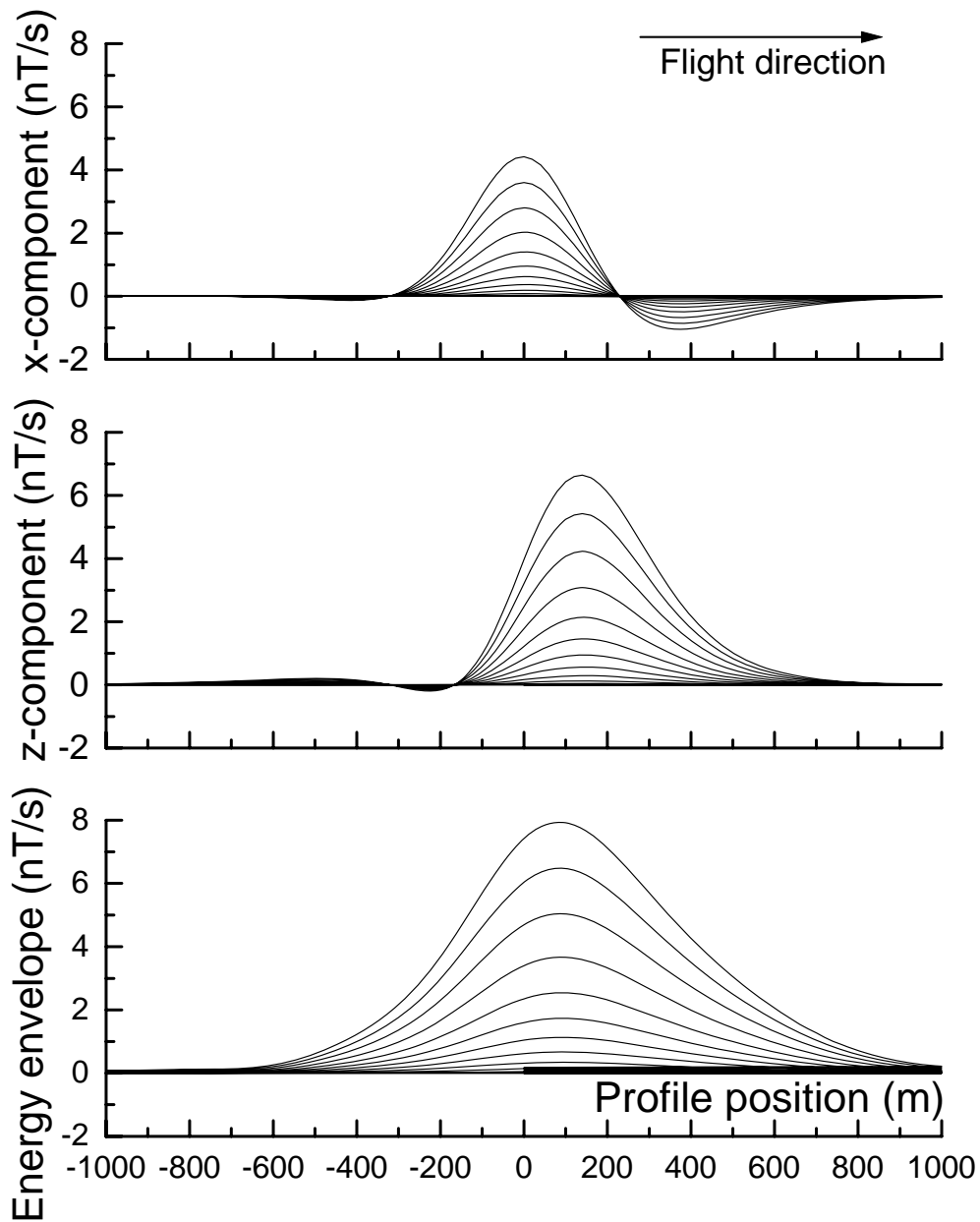


Figure 15: East-dipping plate, depth of 300 m.

Sphere Modeling

The sphere in a uniform field program (Smith and Lee, 2001, Exploration Geophysics, 113-118) has been used to generate synthetic responses over a number of sphere models with varying depth of burial (0, 150 and 300 m). The geometry assumed for the fixed-wing airborne EM system and the waveform are as shown in Figures 1 and 2 above.

In all cases the sphere has a radius of 112 m. As the flight path traverses the center of the sphere, the Y component is zero and has not been plotted.

The conductivity of the sphere is 1 S/m. In cases when the conductivity is different, an indication of how the amplitudes may vary can be obtained from the nomogram that follows (Figure 16).

In the following profile plots (Figures 17 to 19), all components are in nT/s, for a transmitter dipole moment of 900 000 Am². If the dipole moment is larger or smaller, then the response should be scaled up or down appropriately. The plotting point is the receiver location.

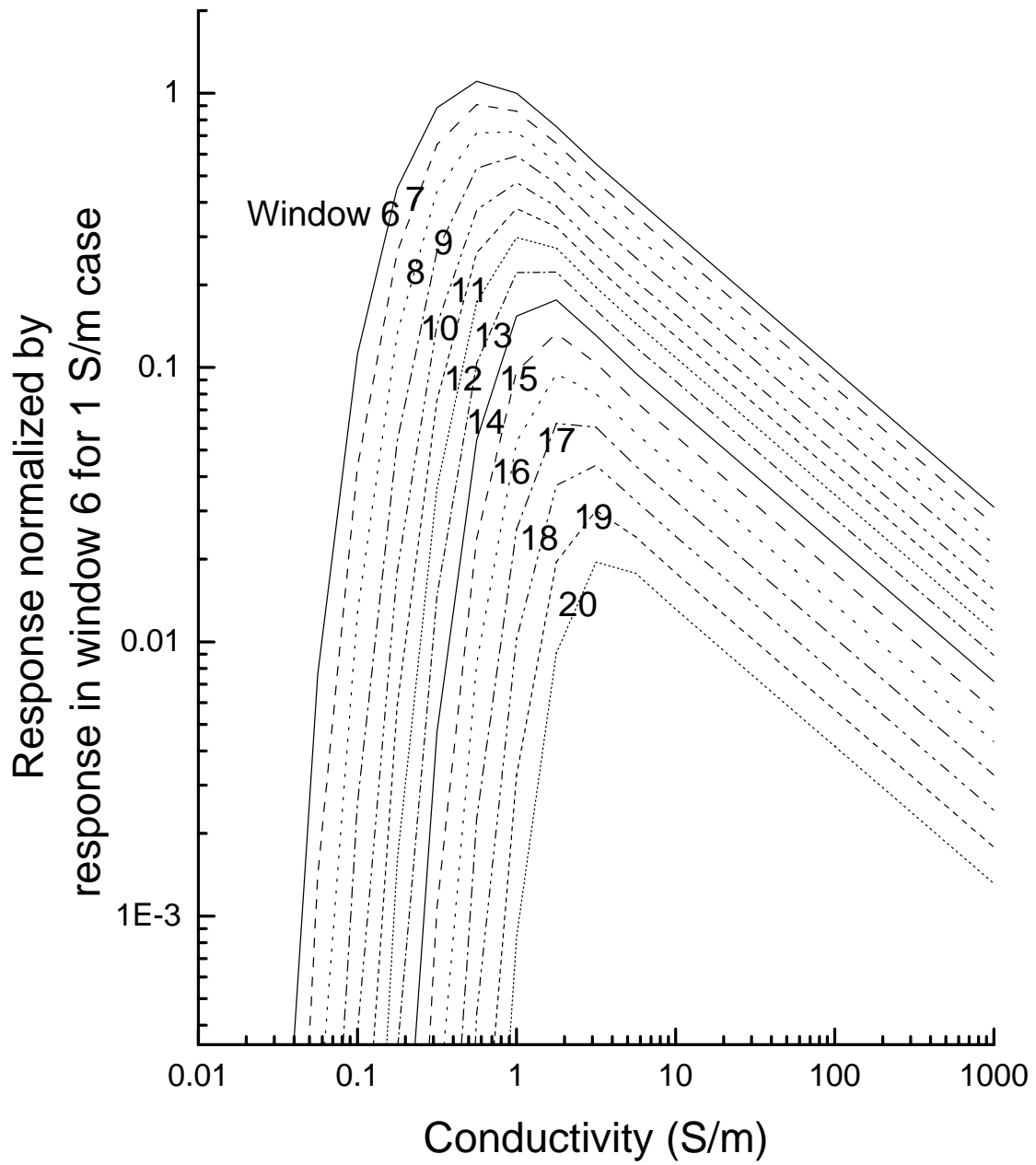


Figure 16: Nomogram for windows 6-20 normalized to a response from a 1 siemen conductor in window 6.

Sphere: depth to top=0

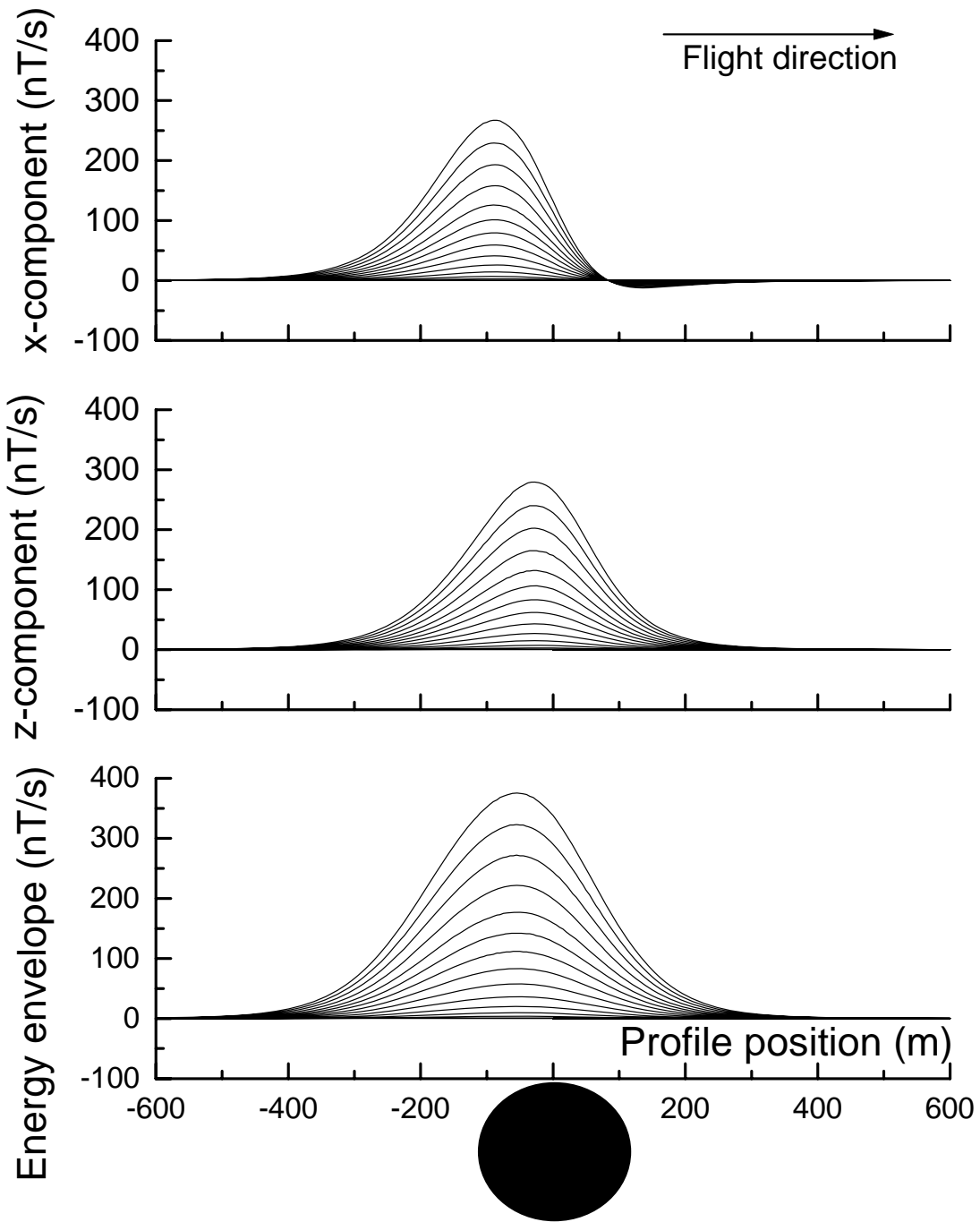


Figure 17: Sphere, depth of 0 m.

Sphere: depth to top=150

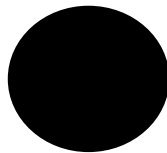
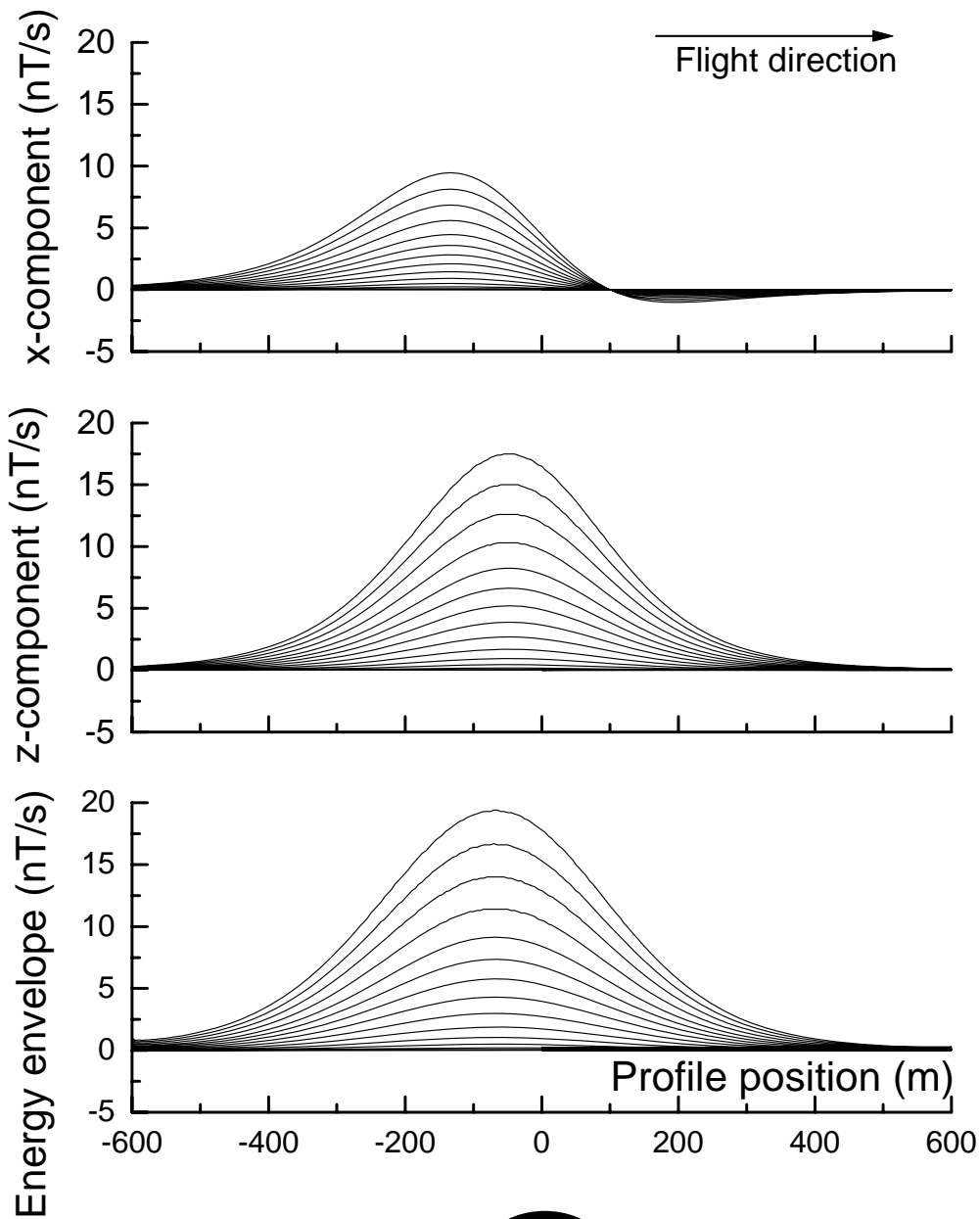


Figure 18: Sphere, depth of 150 m.

Sphere: depth to top=300

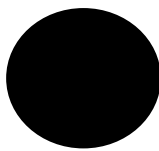
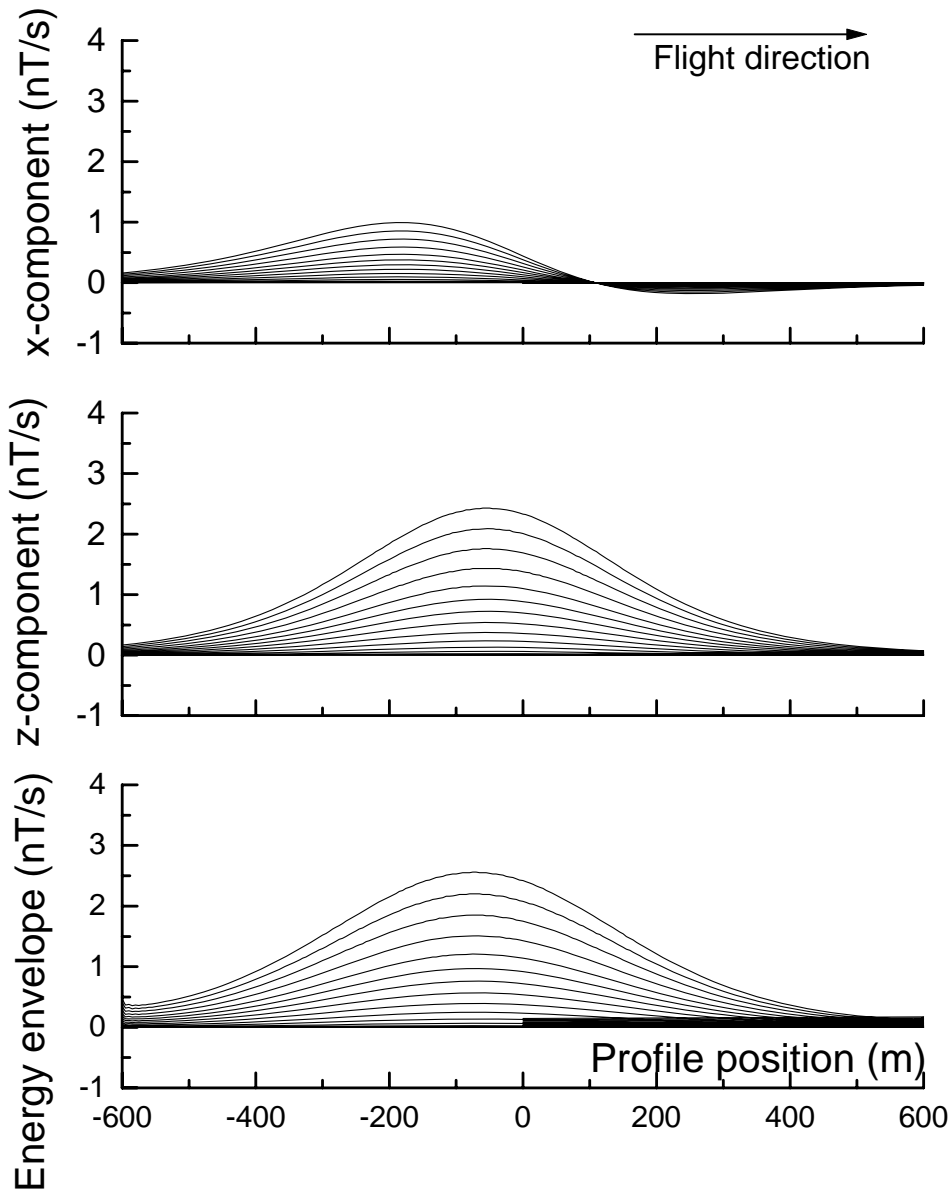


Figure 19: Sphere, depth of 300 m.